Fundamentals of Supported Catalysts for Atom Transfer Radical Polymerization (ATRP) and Application of an Immobilized/Soluble Hybrid Catalyst System to ATRP

Sung Chul Hong and Krzysztof Matyjaszewski*

Center for Macromolecular Engineering, Department of Chemistry, Carnegie Mellon University, 4400 Fifth Avenue, Pittsburgh, Pennsylvania 15213

Received January 11, 2002; Revised Manuscript Received May 1, 2002

ABSTRACT: A series of hybrid catalysts, comprising a tethered ligand immobilized catalyst operating in conjunction with a small amount of soluble catalyst, were evaluated for atom transfer radical polymerization (ATRP). The level of control over the ATRP of vinyl monomers was significantly improved by the addition of part per million levels of a soluble catalyst, or soluble catalyst precursor, to the immobilized catalyst. Use of a hybrid catalyst system for polymerization of vinyl monomers such as MMA, MA, and styrene provided polymers with a predetermined molecular weight and a narrow molecular weight distribution. The immobilized catalyst can be removed from the polymerization by simple filtration, or sedimentation, affording a colorless transparent polymer solution with a salient reduction in the concentration of any residual transition metal in the final polymeric products.

Introduction

Free radical polymerization is widely used in industry for the preparation of an extensive spectrum of materials because of the availability of a wide range of radically polymerizable monomers, mild reaction conditions, and tolerance to impurities such as moisture. The development of controlled/"living" radical polymerizations (CRPs)[1,2] in the 1990s provided a revolutionary broadening of the spectrum of the materials capable of being prepared by radical processes. Through CRP, it became possible to control the molecular weight (MW) and molecular weight distribution (MWD) to prepare polymers that retain chain end-functionality and exhibit well-defined architectures, such as block, graft, or star shaped copolymers, from free radically polymerizable monomers using a free radical polymerization process.

Atom transfer radical polymerization (ATRP)[3] has developed into one of the most robust synthetic tools within the spectrum of CRP processes.[4−9] The basis of ATRP is the reversible transfer of a radically transferable atom, typically a halogen atom, from a monomeric or polymeric alkyl (pseudo)halide to a transition metal complex in a lower oxidation state, forming an organic radical and a transition metal complex in a higher oxidation state. During the early stages of the development of ATRP, equivalent amounts of transition metal complex and monomeric, or polymeric, alkyl halide initiator were typically employed in nonpolar media in order to achieve reasonable polymerization rates. While more active catalysts have now been developed, one of the perceived limitations of ATRP remains the presence of the transition metal catalyst in the polymerization system, which may cause environmental problems that commercial manufacturers would have to address. Therefore, it remained a desirable objective to identify methods that reduced the amount of transition metal used in the process and removed or potentially recycled the metal complex after the polymerization was complete.

* To whom correspondence should be addressed. E-mail: km3b@andrew.cmu.edu.

In addition to development of more active ATRP catalyst systems that allow a significant reduction of the catalyst used in ATRP,[10−16] several postpolymerization purification steps have been evaluated in the laboratory for the removal of a soluble catalyst from a polymer solution. These include precipitation of polymer in nonsolvents, filtration of the polymer solution through aluminum oxide, or treatment with an ion-exchange resin.[17] For in-situ purification of the reaction medium, liquid−liquid phase separation where the metal complex is preferentially located in one phase, has also been demonstrated. For example, systems have been developed and described for separation of catalysts from CO_2 medium,[18] ionic liquids,[19−21] emulsion ATRP,[22−25] and fluorous biphasic conditions.[26] However, these techniques present some scale-up difficulties including cost, loss of polymers, unknown amount of residual metal complex in the polymer, and/or lack of control over the polymerization. One solution to these problems is to use a solid−liquid phase separation such as the immobilization of one of the polymerization components on a support.

Angot et al.[27] immobilized the ATRP initiator group on Wang resins and harvested the polymer chains by hydrolysis of the polymer−resin linkage through postpolymerization treatment. Von Werne et al., and our group, have immobilized ATRP initiators on silica nanoparticles,[28] polysilsesquioxane nanoparticles,[29] or flat silicon surfaces,[30] but these approaches are expensive for production of unattached polymer. The most extensively examined approach has been development of procedures for the immobilization of ATRP catalysts on a solid support, providing a more efficient way of separating and potentially recycling the catalyst. Haddleton et al. immobilized a copper(I) pyridylmethanimine complex[31] on both silica and polystyrene bead through covalent bonding. They also tested a $RuCl_2(PPh_3)_3$ catalyst[32] on a 3-aminopropyl-functionalized silica support through physical adsorption of the catalyst. Kickelbick et al. examined the use of tris(2-aminoethyl)amine and diethylenetriamine ligands attached to a silica support and bispicolylamine ligand

10.1021/ma020054o CCC: $22.00 © 2002 American Chemical Society
Published on Web 08/20/2002

Table 1. Range of Activation and Deactivation Rate Constants with Homogeneous and Immobilized ATRP Catalysts

Activation Rate Constant

	diffusion limit (L mol^{-1} s^{-1})	k_a (L mol^{-1} s^{-1})	$k_{a,overall}$[a] (L mol^{-1} s^{-1})
homogeneous catalyst	$\sim 10^9$	$\sim 10^0$	$\sim 10^0$
immobilized catalyst	$\sim 10^5$	$\sim 10^0$	$\sim 10^0$

Deactivation Rate Constant

	diffusion limit (L mol^{-1} s^{-1})	k_d (L mol^{-1} s^{-1})	$k_{d,overall}$[a] (L mol^{-1} s^{-1})
homogeneous catalyst	$\sim 10^9$	$\sim 10^7$	$\sim 10^7$
immobilized catalyst	$\sim 10^5$	$\sim 10^7$	$\sim 10^5$

[a] $k_{overall} = k_{slowest}$.

Scheme 1

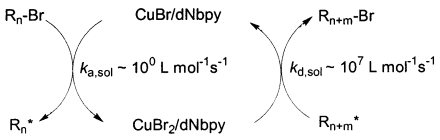

(a)

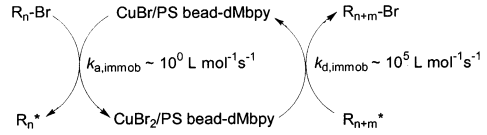

(b)

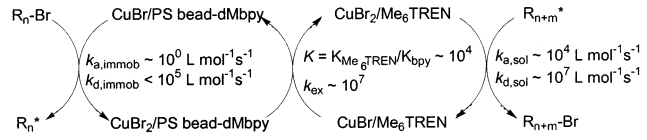

(c)

attached to a polystyrene bead.[33] CuBr/hexamethyltriethylenetetramine (HMTETA) adsorbed on silica[34] was investigated by Shen et al. and was applied to a continuous polymerization process[35] and to the production of a poly(methyl methacrylate) macromonomer using a functionalized initiator.[36] Unfortunately, the heterogeneous nature of these techniques, as presently described, offers limited control over the polymerization (Table 1).

In ATRP systems the activation rate constant (k_a) is typically in the range of $\sim 10^\circ$ L mol^{-1} s^{-1} and the deactivation rate constant (k_d) is in the range of $\sim 10^7$ L mol^{-1} s^{-1} (k_a and k_d in Table 1).[37] In homogeneous ATRP, the overall rates of activation and deactivation are not significantly affected by diffusion, since both oxidation states of the catalyst are readily available ($k_{a,overall} = k_a \sim 10^\circ$ L mol^{-1} s^{-1} and $k_{d,overall} = k_d \sim 10^7$ L mol^{-1} s^{-1}; Table 1 and Scheme 1a). However, for an immobilized catalyst, diffusion of polymer chains to the catalytic complexes attached to a substrate may become rate determining (diffusion limit $\sim 10^5$ L mol^{-1} s^{-1} in Table 1).[33] Diffusion effects therefore significantly lower the overall rate of deactivation because the diffusion limit is much lower than the deactivation rate constant ($k_{d,overall} = k_{diff} \sim 10^5$ L mol^{-1} s^{-1} $\ll k_d \sim 10^7$ L mol^{-1} s^{-1} in Table 1 and Scheme 1b). Almost no effect is seen on the activation step ($k_{a,overall} = k_a \sim 10^\circ$ L mol^{-1} s^{-1} $\ll k_{diff} \sim 10^5$ L mol^{-1} s^{-1} in Table 1 and Scheme 1b).[33] The net result of slow, or insufficient, deactivation of the growing radical is formation of a polymer exhibiting a higher MW than the theoretical one and a broader MWD.

One approach to overcome diffusion limitations is to make the attached catalyst more available to the radical by the use of a spacer between the support and the catalyst complex. Kroell et al. examined the use of a terpyridine ligand grafted onto a silica support through spacers between the carrier surface and the catalytic species,[38] but control over the polymerization was still poor ($M_w/M_n > 1.5$). Shen et al. reported the use of silica gels grafted with ATRP ligands (tetraethyldiethylenetriamine and bispicolylamine) via poly(ethylene glycol) (PEG) spacers to increase the flexibility of the catalyst.[39] A high polymerization rate was obtained using a CuBr based catalyst immobilized on the silica gel, producing PMMA with controlled molecular weights and low polydispersities ($M_w/M_n \sim 1.2-1.4$) when an optimum poly(ethylene glycol) spacer with DP = 3 was employed. The use of a non-cross-linked polyethylene support has also been cited as a soluble/recoverable catalyst carrier to overcome the diffusion limitation. The carrier exhibits reversible solubility properties that allow solubilization of the complex in the reaction medium at the polymerization temperature but precipitation from solution at a lower temperature, allowing recovery.[40] Shen et al. combined the two techniques and used a CuBr/triethyldiethylenetriamine complex attached to a poly(ethylene)-*block*-poly(ethylene glycol), as a soluble/recoverable polyethylene catalyst carrier with a flexible poly(ethylene glycol) spacer.[41] While these systems displayed good control over ATRP, no data on the amount of residual metal complex in polymers was presented.

In a preliminary communication, we reported a "hybrid" catalyst system that was composed of a catalyst immobilized on a particle through an attached ligand and a small amount of soluble catalyst.[42] The hybrid catalyst system was an effective system for controlled ATRP due to acceleration of the deactivation rate of the growing radical through the use of a small amount of low molecular weight soluble catalyst. After the growing radical was deactivated, the soluble catalyst was reconverted to the deactivator Cu(II) species through a rapid halogen exchange reaction with the immobilized catalyst without a significant diffusion barrier. Control over polymerization of vinyl monomers was achieved without sacrificing the main advantage of an immobilized catalyst system, the low concentration of residual metal in polymer (residual Cu $\sim$ 15 ppm). Compared to the other immobilized catalyst systems, the advantage of this technique is its simplicity and versatility, which allows the catalyst designer to select the most appropriate catalyst components for preparation of the targeted material and prepare that material with low residual levels of transition metal in the final polymer. In this paper we will present the initial results of a systematic study of various combinations of the components employed in the immobilized/soluble hybrid catalyst and describe controlled polymerization under a range of conditions. One approach to catalyst regeneration is also discussed.

Experimental Part

Chemicals. Methyl acrylate (MA, 99%, Aldrich), *n*-butyl acrylate (^{n}BuA, 99+%, Acros), methyl methacrylate (MMA, 99%, Aldrich), and styrene (sty, 99%, Aldrich) were passed through a column filled with neutral alumina, dried over CaH_2, distilled under reduced pressure, and stored in a freezer under

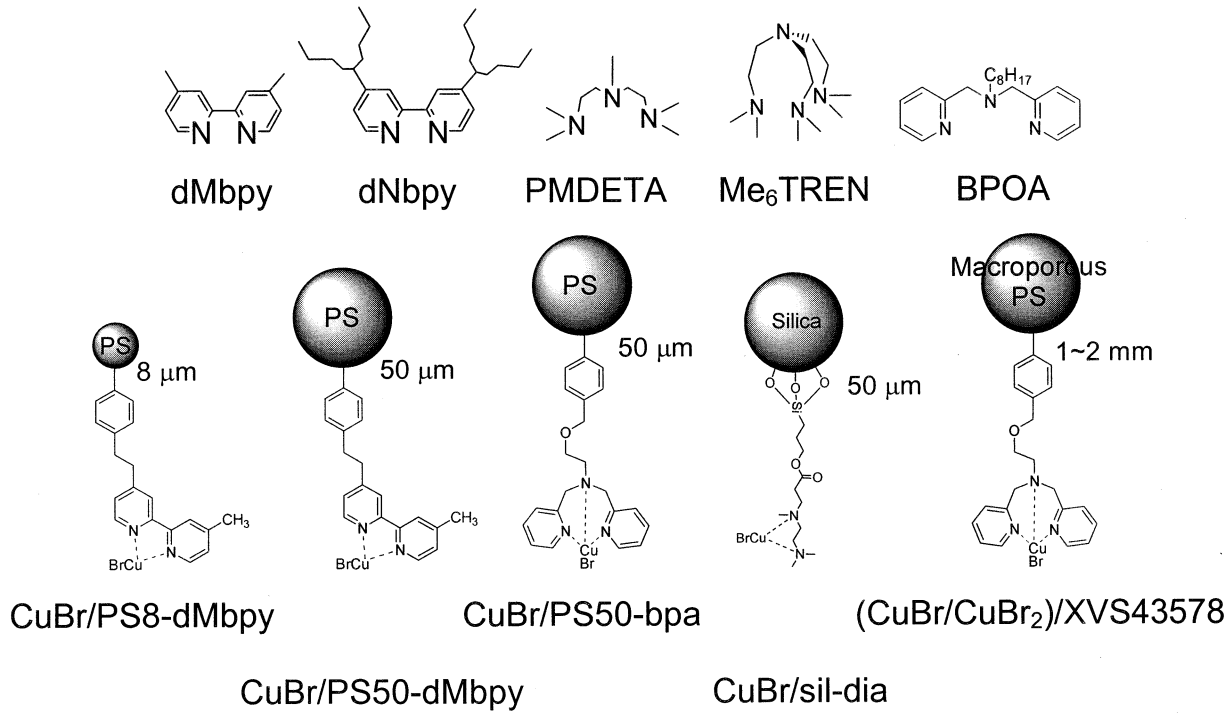

Figure 1. Structures of the ligands and immobilized catalysts.

nitrogen. CuBr (99+%, Aldrich) and CuCl (99+%, Aldrich) were purified by stirring in acetic acid for 5 h followed by washing with ethanol and diethyl ether. Cu^0 powder and Cu^0 wire (bare copper, Fisher) were immersed in glacial acetic acid for 24 h and rinsed with absolute ethanol and diethyl ether immediately before use. Tetrahydrofuran (THF, HPLC grade, Fisher) and toluene (certified grade, Fisher) were freshly distilled from Na/K alloy with benzophenone (99%, Aldrich) and stored under nitrogen. Diisopropylamine (99%, Acros) was distilled from CaH_2 prior to use. 4,4′-Di(*n*-nonyl)-2,2′-bipyridine (dNbpy)[43] and tris(2-(dimethylamino)ethyl)amine (Me_6TREN)[44] were synthesized following previously reported procedures. 4,4′-Dimethyl-2,2′-bipyridine (dMbpy, 99%, Aldrich) was recrystallized from ethanol solution at −15 °C. *N*,*N*,*N*′,*N*″,*N*″-Pentamethyldiethylenetriamine (PMDETA, 99%, Aldrich) was used without further purification. Silica gel (40−60 μm, surface area 548 m^2/g, average pore size 52.7 Å, J&W Scientific) was dried under vacuum at 110 °C for 16 h prior to use. The DOWEX anion-exchange resin XVS43578 (*N*,*N*-bis(2-pyridylmethyl)ethylamine functionalized, 2.26×10^{-3} mol-ligand/g-cat, from DOW Chemical) was washed with distilled water three times and neutralized with 1 M NaOH until the rinsing solution just turned alkaline. The color of the resins changed from yellow to brown. The resin was further washed with distilled water and MeOH and dried under vacuum at 60 °C for 6 h. Poly(styrene-*co*-divinylbenzene) microspheres (PS8, average particle size 8 μm, 5% divinylbenzene, Aldrich), chloromethylated poly(styrene-*co*-divinylbenzene) beads (PS50, average particle size 50 μm, 1% cross-linked, 2.03×10^{-3} mol-Cl/g-bead, Aldrich), $CuBr_2$ (98%, Aldrich), $CuCl_2$ (97%, Aldrich), 2-picolyl chloride hydrochloride (98%, Aldrich), ethanol amine (99+%, Aldrich), *n*-butyllithium (2.5 M solution in hexane, Acros), 3-(trimethoxysilylpropyl)acrylate (92%, Aldrich), *N*,*N*,*N*′-trimethylethylenediamine (97%, Aldrich), 2-bromopropionitrile (97%, Aldrich), 1-bromoethylbenzene (97%, Aldrich), and other solvents were used without further purification. The monomers and solvents were purged by bubbling with dry nitrogen for 1 h immediately before the polymerization. The catalysts and ligands used in this study are presented in Figure 1.

Preparation of CuBr/PS(8 μm)−(4,4′-Dimethyl-2,2′-bipyridine) Immobilized Catalyst (CuBr/PS8-dMbpy). (A) Preparation of Chloromethylated Poly(styrene-*co*-divinylbenzene) Beads (PS8-Cl). A mixture of 11.2 mL of $SnCl_4$ (9.57×10^{-2} mol) and 108.25 mL of $ClCH_2OCH_3$ was added to a slurry of 38.32 g of poly(styrene-*co*-divinylbenzene) beads (PS8, 8 μm beads) in 500 mL of chloroform. The reaction mixture was stirred at room temperature for 4 h. The resulting resin was successively washed with dioxane/water, dioxane/3 N HCl, dioxane, water, and methanol, and dried under vacuum, yielding a resin containing 1.14×10^{-3} mol-Cl/g-cat.

(B) Preparation of PS(8 μm bead)−(4,4′-Dimethyl-2,2′-bipyridine) (PS8-dMbpy). Dry THF (50 mL) and diisopropylamine (10.3 mL, 7.34×10^{-2} mol) were added to a 500 mL flask, which had been purged with N_2 followed by evacuation. The reaction mixture was cooled in a dry ice/acetone bath, and *n*-butyllithium (29.4 mL, 7.34×10^{-2} mol) was slowly added. After addition was complete, the reaction mixture was stirred at −78 °C for 1 h before a solution of dMbpy (13.52 g, 7.34×10^{-2} mol) dissolved in a fresh 120 mL of THF at 60 °C was transferred by cannula to the flask. The reaction was stirred at −78 °C for an additional 1.5 h. In a separate flask, 11.43 g of chloromethylated PS beads (PS8-Cl, 2.45×10^{-2} mol Cl) was suspended in 100 mL of dry THF under nitrogen. The diisopropylamine/*n*-butyllithium/dMbpy solution was transferred to the PS bead suspension by cannula at −78 °C, the reaction temperature was allowed to increase to room temperature, and the reaction mixture was stirred for 78 h. The product was washed with THF five times, methanol five times, and toluene twice, affording 12.86 g of yellow powder containing 1.15×10^{-3} mol-ligand/g-resin as determined by CHN analysis.

(C) Metalation of PS(8 μm bead)−(4,4′-Dimethyl-2,2′-bipyridine) with CuBr (CuBr/PS8-dMbpy). A second sample of PS8-dMbpy resin (1.54 g) and CuBr (0.29 g, 2.0×10^{-3} mol) were introduced into a 100 mL Schlenk flask followed by evacuation with high vacuum and refilling with dehydrated nitrogen three times. THF (80 mL) was then added to the flask to suspend the solids, and the temperature was increased to 60 °C. The reaction mixture was stirred at this temperature for 48 h. The dark brown supported catalyst complex was washed thoroughly with 80 mL of degassed THF three times at 60 °C, followed by washing twice with 80 mL of degassed toluene and twice with 80 mL of degassed hexane, dried under vacuum, and stored under dry nitrogen in a glovebox. CHN analysis indicated 2.4×10^{-3} mol-ligand/g-resin and 1.58×10^{-3} mol-Cu/g-resin by Cu analysis.

(D) Metalation of PS(8 μm)−(4,4′-Dimethyl-2,2′-bipyridine) with $CuBr_2$ ($CuBr_2$/PS8-dMbpy). In a similar manner, a supported $CuBr_2$ complex was formed from 0.9985 g of PS bead (8 μm)−bpy and 0.2565 g of CuBr2 (1.17×10^{-3} mol). The dark brown catalyst, containing 7.46×10^{-4} mol-Cu/g-cat by Cu analysis, was dried under vacuum and stored under dry nitrogen in a glovebox.

Preparation of CuBr/PS(50 μm)−(4,4′-Dimethyl-2,2′-bipyridine) Immobilized Catalyst (CuBr/PS50-dMbpy). A larger particle resin supported catalyst complex, based on 50 μm polystyrene particles, was prepared in the same manner. The commercially available chloromethylated resin was functionalized with 4,4′-dimethyl-2,2′-bipyridine as described above for the PS(8 μm) resin, and a supported metal complex was formed by reaction of 1.5248 g of the PS50-bpy resin with 0.444 g of CuBr (3.17×10^{-3} mol), yielding a black/brown powder containing 1.190×10^{-3} mol-Cu/g-resin from copper analysis.

Preparation of CuBr/PS(50 μm)−(*N*,*N*-Bis(2-pyridylmethyl)ethylamine) Immobilized Catalyst (CuBr/PS50-bpa). (A) Synthesis of *N*,*N*-Bis(2-pyridylmethyl)-2-hydroxyethylamine (BPAOH). Ethanolamine (3.02 mL, 0.05 mol) was added dropwise to solution of 16.4 g of 2-picolyl chloride hydrochloride (0.1 mol) in 80 mL of water. The mixture was stirred and heated to 60 °C, and a solution of NaOH (8 g, 0.2 mol) in 40 mL of water was added dropwise. The resulting red solution was stirred overnight and then cooled to room temperature. The mixture was extracted with chloroform and the extract concentrated by the evaporation of solvent. The residual dark red oil was adsorbed onto basic alumina and then eluted with chloroform. The concentration of the eluted solution gave a light brown oily product (10.26 g, 84.4% yield). ^{1}H NMR ($CDCl_3$) δ 2.89 (t, 2H), 3.67 (t, 2H), 3.92 (s, 4H), 7.13 (dd, 2H), 7.32 (d, 2H), 7.57 (dd, 2H), 8.52 (d, 2H); ESI MS ($M + Na^+$) calculated 266.3, found 266.3; IR cm^{-1} 3000−3500 (OH str), 2700−3000 (CH str), 1800−2300 (aromatic), 1600 (C═N str), 1050 (C−N str).

(B) Preparation of PS(50 μm)−(*N*,*N*-Bis(2-pyridylmethyl)ethylamine) (PS50-bpa). In a glovebox, 0.246 g of BPAOH (1.01 mmol) was dissolved in 10 mL of dry DMF and then 0.024 g of sodium hydride (1.01 mmol) was slowly added to the DMF solution. After stirring for 2 h at room temperature, the mixture was removed from the glovebox and 0.119 g of chloromethylated poly(styrene-*co*-divinylbenzene) bead (PS50, 0.202 mmol) and 7.5 mg of ^{n}Bu4NI (0.020 mmol) were sequentially added to this solution. The mixture was stirred for an additional 48 h at room temperature. The resin was filtered and washed several times with THF, followed by washing with ethyl acetate, methanol, DMF, THF, and diethyl ether. The resin was dried under vacuum for 24 h. Yield: 0.115 g of resin, calculated to contain 1.224×10^{-3} mol-ligand/g-resin from CHN analysis.

(C) Metalation of PS (50 μm)−(*N*,*N*-Bis(2-pyridylmethyl)ethylamine) (CuBr/PS50-bpa). The PS bead (50 μm)−bpa (1.5079 g) was complexed with CuBr (0.3077 g, 2.145×10^{-3} mol) by stirring at 90 °C for 20 h. The resulting light green supported catalyst complex was washed once with 60 mL of DMF, once with THF, and twice with pentane, dried under vacuum, and stored under dry nitrogen. Analysis indicated 1.00×10^{-3} mol-cat/g-resin.

Preparation of CuBr/Silica-(*N*,*N*,*N*′-trimethyl-*N*′-[3-(trimethoxysilylporpoxycarbonyl)ethyl]ethylenediamine) Immobilized Catalyst (CuBr/sil-dia). (A) Synthesis of *N*,*N*,*N*′-Trimethyl-*N*−[3-(trimethoxysilylporpoxycarbonyl)ethyl]ethylenediamine. *N*,*N*,*N*′-Trimethylethylenediamine (6.66 mL, 5.13×10^{-2} mol) was introduced dropwise over a 1 h period to 3-(trimethoxysilylpropyl acrylate) (9.48 mL, 4.27×10^{-2} mol) at 0 °C. The reaction mixture was stirred for a further 30 min at 0 °C, and the temperature was allowed to increase to room temperature, at which the reaction was stirred for a further 47 h. Conversion was checked by the disappearance of the acrylate peak at 6 ppm in ^{1}H NMR analysis. Unreacted *N*,*N*,*N*′-trimethylethylenediamine was removed under high vacuum. ^{1}H NMR ($CDCl_3$) δ 3.90 ppm (t, 2H, COOCH_2); 3.40 ppm (s, 9H, SiOCH_3); 2.60 ppm (t, 2H, CH_2COO); 2.35 ppm (m, 4H, CH_2N); 2.25 ppm (t, 2H, NCH_2-CH_2COO); 2.10 ppm (s, 9H, NCH_3); 1.60 ppm (m, 2H, SiCH_2CH_2); 0.50 ppm (t, 2H, SiCH_2).

(B) Preparation of Silica Supported *N*,*N*,*N*′-Trimethyl-*N*′-[3-(trimethoxysilylporpoxycarbonyl)ethyl]ethylenediamine (sil-dia). Silica (3.87 g) was added under nitrogen to a 250 mL three necked flask, and a solution of 1.95 g of *N*,*N*,*N*′-trimethyl-*N*′-[3-(trimethoxysilylporpoxycarbonyl)ethyl]-ethylenediamine (7.2×10^{-3} mol) in 30 mL of dry THF was added. The reaction was held at 70 °C for 42 h, and all volatiles were removed by application of high vacuum. The product was washed four times with 40 mL of dry, degassed THF, yielding a solid that was analyzed to contain 7.0×10^{-4} mol-ligand/g-solid by CHN analysis.

(C) Metalation of Silica-(*N*,*N*,*N*′-trimethyl-*N*′-[3-(trimethoxysilylporpoxycarbonyl)ethyl]ethylenediamine) (CuBr/sil-dia). The silica supported ligand prepared above (2.322 g of sil-dia) was metalated by reaction with 0.3318 g of CuBr (2.37×10^{-3} mol) by suspension of the silica and transition metal in degassed, dry THF and stirring at 60 °C for 18 h. The THF was removed under vacuum, and the resin was washed four times with 40 mL of dry, degassed THF. The resulting mixture was dried under vacuum, affording a blue powder containing 6.91×10^{-4} mol-Cu/g-solid complex from copper analysis.

Preparation of DOWEX Resins Complexed with CuBr/$CuBr_2$. Metalation of DOWEX Resin XVS43578 with CuBr/$CuBr_2$. A mixture of 4.8184 g of neutralized DOWEX resin, 0.6942 g of CuBr, and 0.2703 g of $CuBr_2$ ([ligand in resin]/[CuBr]/[$CuBr_2$] = 1:0.8:0.2) was introduced into a 100 mL Schlenk flask, and oxygen was removed by degassing under vacuum and backfilling three times with N_2. Dry, degassed THF (50 mL) was added, and the temperature was increased to 70 °C. The reaction mixture was stirred further for 24 h. The resulting supported catalyst complex was washed with 80 mL of degassed THF three times and twice with 80 mL of degassed pentane. The catalyst resin was dried under vacuum and stored under dry nitrogen. Copper analysis indicated 5.90×10^{-4} mol-Cu/g-resin (Figure 1).

Polymerization. In a typical polymerization procedure the supported catalyst complex, CuBr/PS8-dMbpy (0.07 g, 5.20×10^{-5} mol-Cu/g-cat), was placed in a 50 mL Schlenk tube followed by degassing under vacuum and backfilling three times with N_2. A mixture of degassed monomer MMA (1.67 mL, 1.560×10^{-2} mol), toluene (1.47 mL), anisole (0.2 mL), and $CuBr_2$/Me_6TREN (5.2×10^{-7} mol) (0.22 mL, from a stock solution of $CuBr_2 = 2.38 \times 10^{-5}$ mol and $Me_6TREN = 2.38 \times 10^{-5}$ mol, in acetone, 10 mL) was then added. A measured amount of initiator (2-bromopropionitrile, 4.50×10^{-3} mL, 5.2×10^{-5} mol) was added, and the reactor was immersed in an oil bath that was preset to the specific reaction temperature (90 °C). Samples were taken from the flask via syringe at timed intervals to allow kinetic data to be determined. The samples were immediately diluted with THF and filtered through a Gelman Acrodisc PTFE filter (0.2 μm) for the analyses, including gas chromatography (GC) and gel permeation chromatography (GPC). After a certain polymerization time, the polymerization system was removed from the oil bath and cooled to room temperature. The polymer solution was diluted with THF, filtrated through a Gelman Acrodisc PTFE filter (0.2 μm), and kept at room temperature for further analysis.

Regeneration of Immobilized Catalyst. A sample of immobilized catalyst (0.3 g) from previous polymerizations was collected and washed five times with 60 mL of degassed THF. The resin was added to a Schlenk tube along with 20 mL of degassed THF, two pieces of Cu^0 wire which had been washed with acetic acid prior to use, and $CuBr_2$/Me_6TREN (2.26×10^{-5} mol, or 10 mol % Cu to that in immobilized catalyst). The mixture was stirred at 60 °C for 24 h. The color of the immobilized catalyst changed from light brown to dark/red brown over a 6 h period as the Cu^0 was transported from the wire to the resin by the action of the soluble Me_6TREN ligand. The regenerated immobilized catalyst was washed with 20 mL of degassed THF three times, dried under vacuum, and kept under nitrogen.

Table 2. Methyl Methacrylate, Methyl Acrylate, and Styrene Polymerization with CuBr/PS8-dMbpy, $CuBr_2/Me_6TREN$, and the Corresponding Hybrid Catalysts[a]

expt no.	monomer	hybrid ratio[b] (mol %)	$w_0(Cu_{sol})/w_0$(monomer)[c] (ppm)	polym time (h)	conv[d] (%)	M_n ($\times 10^3$)	M_n(th) ($\times 10^3$)	M_w/M_n	$w(Cu_{sol})/w$(polym)[e] (th, ppm)	$w(Cu_{sol})/w$(polym)[f] (meas, ppm)
1	MMA	0	0	16	59.0	71.2	17.7	2.26	0	<1
2	MMA	100	2182	6	72.1	52.5	21.7	1.95	3026	1730[g]
3	MMA	3	63	24	83.0	26.8	25.0	1.19	76	107
4	MMA	1	21	17	89.1	32.4	26.7	1.25	24	27
5	MMA	0.3	6	24	96.9	35.5	29.0	1.29	6	15
6[h]	MMA	1	21	5.5	91.6	14.3	9.2	1.32	23	29
7[i]	MMA	1	21	5.5	92.5	40.0	27.7	1.58	23	63
8	MA	1	25	51	84.7	21.5	22.6	1.09	30	36
9[h]	MA	1	25	6	96.0	9.7	8.3	1.15	26	39
10	sty	1	20	8	51.9	15.0	15.6	1.26	39	15

[a] Polymerization conditions: initiator = 2-bromopropionitrile except for expt no. 10; for expt. no. 1, $[MMA]_0/[I]_0/[catalyst]_0 = 300:1:1$, $[MMA]_0 = 4.69$ mol/L, MMA/toluene = 1/1 v/v, temperature = 90 °C; for expt no. 2, $[MMA]_0/[I]_0/[CuBr/Me_6TREN]_0/[CuBr_2/Me_6TREN]_0 = 300:1:1:0.03$, $[MMA]_0 = 4.69$ mol/L, MMA/(toluene + anisole)/acetone = 1/1/0.13 v/v/v, temperature = 90 °C, catalyst was partially dissolved; for expt nos. 3 and 4, $[MMA]_0/[I]_0/[CuBr/PS8\text{-}dMbpy]_0 = 300:1:1$, $[MMA]_0 = 4.67$ mol/L, MMA/toluene = 1/1 v/v, temperature = 90 °C; for expt no. 5, $[MMA]_0/[I]_0/[CuBr/PS8\text{-}dMbpy]_0 = 300:1:1$, $[MMA]_0 = 4.67$ mol/L, $CuBr_2/Me_6TREN$ from stock solution in acetone, MMA/toluene/acetone = 1/0.75/0.25 v/v/v, temperature = 90 °C; for expt no. 6, $[MMA]_0/[I]_0/[CuBr/PS8\text{-}dMbpy]_0 = 100:1:1$, $[MMA]_0 = 3.90$ mol/L, $CuBr_2/Me_6TREN$ from stock solution in acetone, MMA/(toluene + anisole)/acetone = 1/1/0.39 v/v/v, temperature = 90 °C; for expt no. 7, $[MMA]_0/[I]_0/[CuBr/PS8\text{-}dMbpy]_0 = 300:1:1$, $[MMA]_0 = 4.68$ mol/L, $CuBr_2/Me_6TREN$ from stock solution in acetone, MMA/(toluene + anisole)/acetone = 1/1/0.13 v/v/v, temperature = 90 °C; for expt no. 8, $[MA]_0/[I]_0/[CuBr/PS8\text{-}dMbpy]_0 = 300:1:1$, $CuBr_2/Me_6TREN$ from stock solution in acetone, $[MA]_0 = 5.55$ mol/L, MA/toluene/acetone = 1/0.87/0.13 v/v/v, temperature = 70 °C; for expt no. 9, $[MA]_0/[I]_0/[CuBr/PS8\text{-}dMbpy]_0 = 100$: 1:1, $[MA]_0 = 5.55$ mol/L, $CuBr_2/Me_6TREN$ from stock solution in acetone, MA/(toluene + anisole)/acetone = 1/1/0.46 v/v/v, temperature = 70 °C; for expt no. 10, initiator = 1-bromoethylbenzene, $[styrene]_0/[I]_0/[CuBr/PS8\text{-}dMbpy]_0 = 300:1:1$, $CuBr_2/Me_6TREN$ from stock solution in acetone, $[styrene]_0 = 4.36$ mol/L, styrene/chlorobenzene/acetone = 1/0.75/0.12 v/v/v, temperature = 110 °C. [b] $[CuBr_2/Me_6TREN]_0/[CuBr/bpy$ immobilized on PS bead$]_0$ (mol %). [c] Initial copper (Cu) content as a soluble catalyst ($CuBr_2/Me_6TREN$ and/or $CuBr/Me_6TREN$) by weight in monomer. [d] Conversion determined by GC. [e] Theoretical residual copper (Cu) content in polymer by weight = $[w_0(Cu_{sol})/w_0$(monomer)]/conversion. [f] Residual copper (Cu) content in polymer by weight determined by inductively coupled plasma (ICP) analysis. [g] The residual amount of copper (Cu) was much less than the theoretical value, probably because of the incomplete dissolution of $CuBr/Me_6TREN$ and $CuBr_2/Me_6TREN$ in the reaction medium. [h] The targeted degree of polymerization is 100. [i] Polymerization performed in the presence of Cu^0 wire.

Characterization. Conversion of monomer was determined using a Shimadzu GC 14-A gas chromatograph equipped with a FID detector using a J&W Scientific 30 m DB WAX Megabore column and anisole as an internal standard. Injector and detector temperatures were kept constant at 250 °C. Analysis was run isothermally at 35 °C for 4 min followed by an increase of temperature to 120 °C at the heating rate 40 °C/min and holding at 120 °C for 1 min. ^1H NMR measurement was performed using a Bruker 300 MHz instrument with $CDCl_3$ as a solvent. UV−visible and IR measurements were performed using a Perkin-Elmer UV/VIS/NIR Lambda 900 spectrometer and an ATI Mattson FTIR, respectively. C, H, N elemental analysis was carried out by Midwest Microlab, Indianapolis, IN. Cu elemental analysis was made by inductively coupled plasma (ICP) by Chemisar Laboratories, Canada. Electrospray ionization (ESI) MS was conducted using a Finnegan LCQ, equipped with an octupole and an ion trap mass analyzer. The morphology of the catalysts was observed by Boder Scientific optical microscope. The molecular weight and molecular weight distribution of polymers were determined by GPC using PSS columns (styrogel 10^5, 10^3, 10^2 Å) equipped with a Waters 515 liquid chromatograph pump and a Waters 2410 differential refractometer with diphenyl ether as an internal standard. THF was used as an eluent at the flow rate 1 mL/min. Linear PMMA standards (960 g/mol ~ 1.577×10^6 g/mol) were used for calibration of methacrylate polymers. Theoretical molecular weights were calculated following eq 1.[8]

$$M_{n,th} = ([\text{monomer}]_0/[\text{initiator}]_0) \times \text{conversion} \times \text{MW(monomer)} \quad (1)$$

The residual concentration of Cu in the polymer was measured by inductively coupled plasma (ICP) by Chemisar Laboratories, Canada. The polymer solution from a polymerization was filtered through a Gelman Acrodisc PTFE filter (0.2 μm), cast onto a glass plate, and dried under vacuum at 60 °C for 12 h, providing a colorless polymer film for Cu analysis.

Results and Discussion

Immobilized/Soluble Hybrid Catalyst and Proposed Mechanism. The overall action of the hybrid catalyst system is depicted in Scheme 1. Since the activation rate constant of dormant/initiating alkyl halide in the ATRP process is in the range $k_a \sim 10^\circ$ L mol^{-1} s^{-1} (Table 1),[37] the activation should not be affected by a slow diffusion of the polymeric chains to the solid immobilized catalyst ($k_{diff} \sim 10^5$ L mol^{-1} s^{-1}, Scheme 1b, Table 1).[33]

The major factor controlling polymerization when using an immobilized catalyst system is the deactivation step, which is affected by both the mobility of the particles carrying the immobilized catalyst and the diffusion of the polymer chains in the reaction mixture. While a homogeneous catalyst does not suffer from any diffusion barrier between higher oxidation state catalyst complex and growing radical, an immobilized catalyst attached to a bulky carrier hinders diffusion of the growing chain end to the catalytic site. Diffusion to a surface therefore may become the rate-determining step. This would result in a low apparent deactivation rate constant for an immobilized catalyst. This behavior is seen in the polymerization of methyl methacrylate (MMA) over a CuBr/PS8-dMbpy immobilized catalyst. The polymer exhibited a large difference between experimental and theoretical molecular weights and had a broad molecular weight distribution (experiment 1 in Table 2, $M_w/M_n = 2.26$). GPC curves did not show a distinct shift of MW with conversion, indicating that a redox initiated polymerization had occurred (Figure 2a).

$CuBr/Me_6TREN$ is known to be an active catalyst system for the polymerization of *n*-butyl acrylate (^{n}BuA) and styrene, allowing the use of significantly lower amounts of catalyst.[12,44] However, when $CuBr/Me_6$-TREN is used for polymerization of MMA, poor control was observed, even at higher concentrations of catalyst,[44] as shown in experiment 2 in Table 2. The polymers were of higher molecular weight than predicted, possessed a broad molecular weight distribution

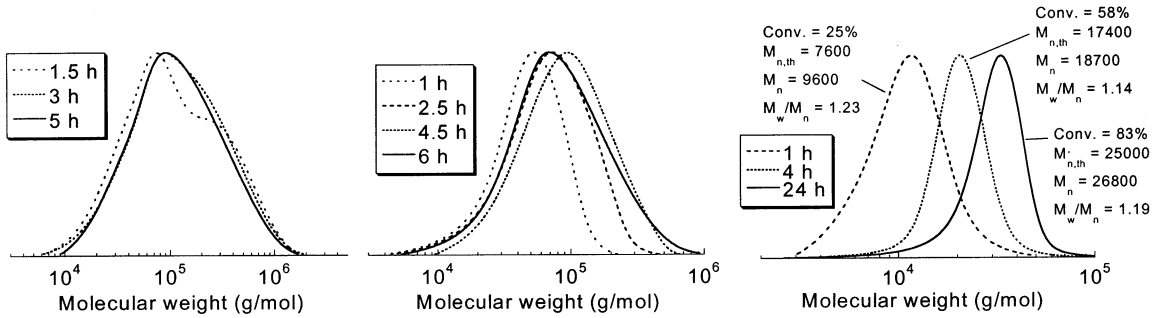

Figure 2. GPC traces from the polymerization of MMA with CuBr/PS8-dMbpy (a, experiment 1 in Table 2); (CuBr/$CuBr_2$)/Me_6-TREN (b, experiment 2 in Table 2); and (CuBr/PS8-dMbpy)/($CuBr_2$/Me_6TREN) hybrid catalyst system (c, experiment 3 in Table 2). See Table 2 for polymerization conditions.

(M_w/M_n = 1.95), and did not show an increase in molecular weight with conversion (Figure 2b).

When a small amount of $CuBr_2$/Me_6TREN catalyst (~3 mol %) was added to the CuBr/PS8-dMbpy immobilized catalyst, the level of control attained in the polymerization was significantly improved (experiment 3 in Table 2 and in Figure 2c). There was a clear increase of molecular weight with conversion and good correlation between theoretical and experimental molecular weights (Figure 2c), and the polymers possessed a narrow molecular weight distribution (M_w/M_n = 1.14 to 1.23), indicating a well-controlled polymerization using the hybrid catalyst system.

$CuBr_2$/Me_6TREN was chosen as the soluble catalyst component for the hybrid system because of its high deactivation rate constant ($k_d = 1.4 \times 10^7$ L mol^{-1} s^{-1}, at 75 °C in acetonitrile)[37] and, perhaps more importantly, because of its overall high reducing power compared to that of Cu/PS8-dMbpy. If we assume that the chemical reactivities of free dMbpy and dMbpy tethered to PS beads are similar, the ratio of the corresponding equilibrium constants can be estimated from the untethered chemical analogue 2,2′-bipyridine (bpy) (eq 2), resulting in $K \sim 10^{4\pm1}$ by UV−vis analysis in methanol[45] and by cyclic voltametry[46] in acetonitrile at 25 °C.

$$Cu^{II}Br_2/bpy + Cu^{I}Br/sol.\text{-}ligand \underset{K_1}{\overset{K_2}{\rightleftarrows}} Cu^{I}Br/bpy + Cu^{II}Br_2/sol.\text{-}ligand \quad (2)$$

This indicates that a dynamic halogen exchange reaction between tethered $CuBr_2$/PS8-dMbpy and soluble CuBr/Me_6TREN occurs to predominantly yield tethered CuBr/PS8-dMbpy and soluble $CuBr_2$/Me_6TREN. The $CuBr_2$/Me_6TREN therefore remains available to rapidly deactivate growing radicals because of this halogen exchange reaction (Scheme 1c). Overall, the $CuBr_2$/Me_6-TREN soluble catalyst acts as a "shuttling" agent that delivers the halogen from the solid immobilized catalyst to growing polymeric radicals, thus overcoming the diffusion barriers and facilitating an effective deactivation process (Scheme 1c).

MMA polymerizations were also conducted with lower concentrations of soluble catalyst (experiments 4 and 5 in Table 2, Figure 3). When $CuBr_2$/Me_6TREN was added at 1 mol % and 0.3 mol % immobilized CuBr/PS8-dMbpy catalyst, which correspond to 24 and 6 ppm of Cu versus monomer by weight, the kinetic curves initially showed a fast rate of polymerization, which then slowed and

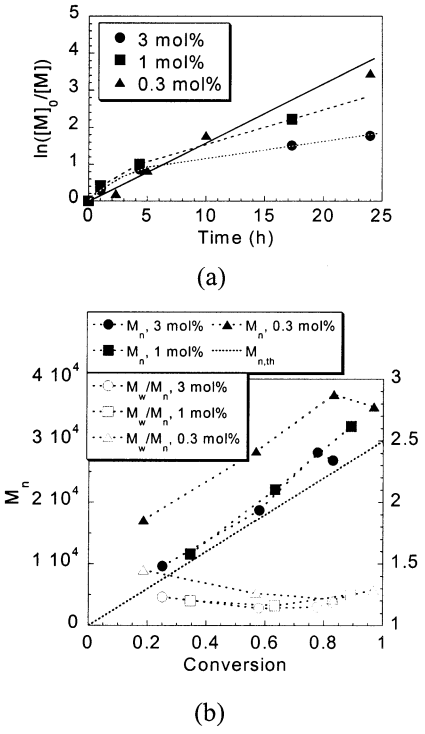

Figure 3. Kinetic plots (a) and evolution of M_n and M_w/M_n vs conversion (b) for the polymerization of MMA using the (CuBr/PS8-dMbpy)/($CuBr_2$/Me_6TREN) hybrid catalyst system with different amounts of $CuBr_2$/Me_6TREN: 3 mol % $CuBr_2$/Me_6-TREN vs CuBr/PS8-dMbpy (● or ○); 1 mol % $CuBr_2$/Me_6TREN vs CuBr/PS8-dMbpy (■ or □); 0.3 mol % $CuBr_2$/Me_6TREN vs CuBr/PS8-dMbpy (▲ or △). see Table 2 for polymerization conditions.

followed first-order kinetics (Figure 3a). The polymerization kinetics became more linear as the amount of soluble CuBr/Me_6TREN decreased because of build up of $CuBr_2$ on the support, changing the equilibrium between CuBr/Me_6TREN and $CuBr_2$/Me_6TREN. The conversion of the monomer essentially reached ~70% in 5 h and ~90% in 20 h. The evolution of M_n with conversion showed good agreement with theoretical molecular weight, which confirmed good control over polymerization along with a narrow molecular weight distribution (Figure 3). Better agreement between the experimental and theoretical molecular weights was observed with higher concentration of soluble catalyst (Figure 3b); however, even with 0.3 mol % $CuBr_2$/Me_6-TREN present versus immobilized catalyst (6 ppm of Cu versus polymer by weight), the molecular weight increased linearly with narrow molecular weight dis-

Table 3. Halogen Exchange Equilibrium Constant (K), Concentration, Activation Rate Constant (k_a), Deactivation Rate Constant (k_d), the Relative Contributions to the Activation ($F_{a,sol}$) and Deactivation Steps ($F_{d,sol}$) of the Soluble Catalysts and the Rate of Polymerization for the Hybrid Catalyst Systems[a]

soluble catalyst	K[b] (K_1/K_2)	[Cu^IBr/sol.-ligand][c] (mol/L)	[$Cu^{II}Br_2$/sol.-ligand][c] (mol/L)	[Cu^{II}/sol]/[Cu^I/sol] (%)	$k_{a,sol}$[d] (L mol^{-1} s^{-1})	$k_{d,sol}$[e] (L mol^{-1} s^{-1})	$F_{a,sol}$[f] (%)	$F_{d,sol}$[g] (%)	R_p[h] ($\times 10^{-3}$ mol L^{-1} s^{-1})
$Cu^{I/II}/Me_6TREN$	$\sim 10^4$	10^{-6}	10^{-4}	99.0	10^3	1.4×10^7	54.1	99.3	7.30
$Cu^{I/II}$/PMDETA	~ 10	10^{-4}	2×10^{-5}	16.7	0.12	6.1×10^6	1.4	92.4	10.37
$Cu^{I/II}$/dNbpy	~ 1	10^{-4}	10^{-6}	1.0	0.085	2.5×10^7	1.0	71.4	11.91
$Cu^{I/II}$/dMbpy	~ 1	10^{-4}	10^{-6}	1.0					

[a] Monomer = methyl methacrylate, immobilized catalyst = PS8-dMbpy. [b] $K = ([Cu^{II}{}_{sol}][Cu^{I}{}_{PS8-dMbpy}])/([Cu^{I}{}_{sol}][Cu^{II}{}_{PS8-dMbpy}]) = K_1/K_2$.[45] [c] Calculated from $K = [Cu^{II}{}_{sol}][Cu^{I}{}_{PS8-dMbpy}]/[Cu^{I}{}_{sol}][Cu^{II}{}_{PS8-dMbpy}]$ when [Cu^IBr/PS8-dMbpy] = 10^{-2} mol/L, [$Cu^{II}Br_2$/PS8-dMbpy] = 10^{-4} mol/L, the total concentration of Cu species is $\sim 10^{-2}$ mol/L, 1 mol % $Cu^{II}Br_2$/sol-ligand is added, and total 2 mol % Cu^{II} species is present. [d] Activation rate constants measured at 35 °C in acetonitrile with 1-bromoethylbenzene.[37] [e] Deactivation rate constants measured at 75 °C in acetonitrile with 1-phenylethyl radical.[37] [f] $F_{a,sol} = R_{act,sol}/(R_{act,sol} + R_{act,immob}) = ([Cu^IBr/sol\text{-}ligand]k_{a,sol})/([Cu^IBr/sol\text{-}ligand]k_{a,sol} + [Cu^IBr/PS8\text{-}dMbpy]k_{a,immob})$; [$Cu^I$Br/PS8-dMbpy] = 10^{-2} mol/L and $k_{a,immob} = 0.085$ L mol^{-1} s^{-1} are used. [g] $F_{d,sol} = R_{deact,sol}/(R_{deact,sol} + R_{deact,immob}) = ([Cu^{II}Br_2/sol\text{-}ligand]k_{d,sol})/([Cu^{II}Br_2/sol\text{-}ligand]k_{d,sol} + [Cu^{II}Br_2/PS8\text{-}dMbpy]k_{a,immob})$; [$Cu^{II}Br_2$/PS8-dMbpy] = 10^{-4} mol/L and $k_{d,immob} = k_{diff} = 10^5$ L mol^{-1} s^{-1} are used. [h] $R_p = k_pK_{eq}[initiator]_0([Cu^I]/[Cu^{II}X])[M] = R_{p,sol} + R_{p,immob}$: $k_p = 1050$ L mol^{-1} s^{-1} at 70 °C;[50,52] $[initiator]_0 = 0.0156$ mol/L; [M] = 4.69 mol/L; $K_{eq,sol} = 7 \times 10^{-7}$ for dNbpy and dMbpy, 10^{-5} for PMDETA, 10^{-3} for Me_6TREN at 100 °C;[44] and $K_{eq,immob} = k_{a,immob}/k_{d,immob} \sim 0.085/10^5 = 8.5 \times 10^{-7}$ are used.

tribution ($M_w/M_n \sim 1.3$), indicating a good control over the polymerization, although a difference between experimental and theoretical molecular weight was noted. This difference between observed and actual MW can also be attributed to the dynamics of the equilibrium between Cu(I) and Cu(II) in solution and on the support. At the early stages of the reaction, there is a significant amount of uncontrolled coupling between small molecules and initiator is consumed in order to set up conditions for controlled polymerization. This behavior can be circumvented by addition of $CuBr_2$ to the solid support.

Other Soluble Catalyst Components in Hybrid Catalyst Systems. $CuBr_2$/4,4′-dimethyl-2,2′-bipyridine (dMbpy), $CuBr_2$/4,4′-di(5-nonyl)-2,2′-bipyridine (dNbpy), and $CuBr_2$/pentamethyldiethylenetriamine (PMDETA) were also evaluated as soluble catalyst components in hybrid catalyst systems for MMA polymerization in conjunction with PS8-dMbpy immobilized catalyst. Polymerization conducted with ($CuBr_2$/dMbpy) and ($CuBr_2$/dNbpy) as soluble component displayed poor control over the polymerization. The level of control over the MMA polymerization was significantly improved by using (CuBr/PS8-dMbpy)/($CuBr_2$/PMDETA) hybrid catalyst systems. The molecular weight distribution was narrow ($M_w/M_n \sim 1.3$), and there was a linear increase of molecular weight with good agreement with theoretical molecular weight. The best results were obtained with (CuBr/PS8-dMbpy)/($CuBr_2$/Me_6TREN). The polydispersity was as low as $M_w/M_n \sim 1.2$. The molecular weight increased linearly with conversion and exhibited good agreement with theoretical molecular weight.

We believe that the differences between the hybrid catalyst systems with these soluble catalyst components originate from differences in the equilibrium constant ($K = [Cu^{II}{}_{sol}][Cu^{I}{}_{PS8-dMpy}]/[Cu^{I}{}_{sol}][Cu^{II}{}_{PS8-dMpy}] = K_1/K_2$) for the halogen exchange reaction with CuBr/PS-dMbpy immobilized catalyst (eq 2). Table 3 lists the estimated K values and shows that Me_6TREN is the most reducing complex of the four soluble Cu complexes, resulting in a very high equilibrium constant $K > 10^4$, followed by Cu complexes with PMDETA ($K \sim 10$, Table 3). K values for $Cu^{I/II}$/dNbpy and $Cu^{I/II}$/dMbpy are essentially unity because of the similar chemical nature of the species (dNbpy and dMbpy versus bpy).[45] This indicates that the equilibrium in eq 2 shifts strongly to the right-hand side when $Cu^{I/II}/Me_6$TREN and $Cu^{I/II}$/PMDETA are used as the soluble catalyst component of the hybrid catalyst, meaning that a dynamic halogen exchange reaction between immobilized and soluble catalyst has occurred. The concentrations of soluble catalyst species ([Cu^IBr/sol.-ligand] and [$Cu^{II}Br_2$/sol.-ligand] in Table 3) were estimated using individual K values assuming the total concentration of Cu species is 10^{-2} mol/L, 1 mol % of soluble catalyst was added, and atotal 2% Cu^{II} species was present. These values indicate that more than 99% of $Cu^{I/II}/Me_6$TREN and 16.7% for $Cu^{I/II}$/PMDETA are in the form of Cu^{II} but that only 1% of $Cu^{I/II}$/dMbpy and $Cu^{I/II}$/dNbpy are in the form of Cu^{II} because of the large excess of tethered Cu^IBr/PS8-dMbpy in the system ([Cu^IBr/PS8-dMbpy] = 10^{-2} mol/L). Since no precise data on the activation and deactivation rate constants for MMA polymerization are available in the literature, we used individual $k_{a,sol}$ and $k_{d,sol}$ values[37] from 1-phenylethyl derivatives for the estimation of the fraction of activation and deactivation reaction performed by the soluble catalyst in the hybrid catalyst system ($F_{a,sol}$ and $F_{d,sol}$ in Table 3). With $Cu^{I/II}/Me_6$TREN, approximately 54% of the activation reaction ($F_{a,sol}$ for $Cu^{I/II}/Me_6$TREN) was provided by the soluble catalyst while 99.3% of the deactivation reaction was accomplished ($F_{d,sol}$ for $Cu^{I/II}/Me_6$TREN in Table 3). This indicated that essentially all deactivation was executed by the small amount ($\sim$1 mol %) of $CuBr_2/Me_6$TREN added. With $Cu^{I/II}$/PMDETA, only 1% of activation ($F_{a,sol}$ for $Cu^{I/II}$/PMDETA in Table 3) was accomplished by the soluble catalyst, because of the large excess of immobilized catalyst ($\sim 10^{-2}$ mol/L, 100 times excess) and similar activation rate constants (0.12 L mol^{-1} s^{-1} for CuBr/PMDETA vs 0.085 L mol^{-1} s^{-1} for CuBr/dNbpy). However, $\sim$92.4% of the deactivation process ($F_{d,sol}$ for $Cu^{I/II}$/PMDETA in Table 3) was catalyzed by the soluble catalyst component ($CuBr_2$/PMDETA) because the immobilized catalyst could not effectively mediate the deactivation process (diffusion limited, $k_d = k_{diff} \sim 10^5$ L mol^{-1} s^{-1}). The situation was similar for $Cu^{I/II}$/dNbpy, where $\sim$1.0% of the activation step was conducted by the soluble component ($F_{a,sol}$ for $Cu^{I/II}$/dNbpy in Table 3) but there was a much lower contribution to the deactivation step, $\sim$71.4% ($F_{d,sol}$ for $Cu^{I/II}$/dNbpy in Table 3). The overall polymerization rates (R_p) for each system were similar (R_p in Table 3), and this was confirmed experimentally (Figure 4a).

Addition of the Uncomplexed Me_6TREN. Other improvements in the polymerization procedures can result from the high binding constant of Cu^{II} species with Me_6TREN in aqueous solution ($K_c \sim 10^{15.4}$).[47] This

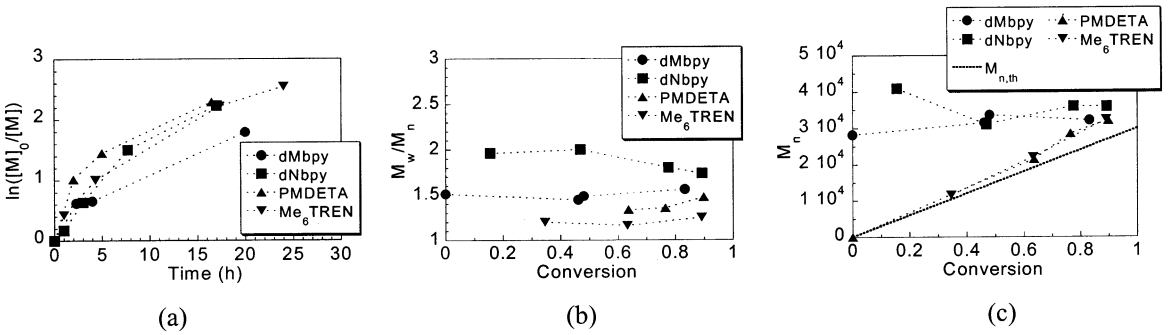

Figure 4. Kinetic plots (a), evolution of M_w/M_n (b), and M_n (c) vs conversion for the polymerization of MMA using the hybrid catalyst system composed of CuBr/PS8-dMbpy as an immobilized catalyst with different soluble catalyst constituents: $CuBr_2$/dMbpy (●); $CuBr_2$/dNbpy (■); $CuBr_2$/PMDETA (▲); $CuBr_2$/Me_6TREN (▼). Polymerization conditions: $[MMA]_0$/[2-bromopropionitrile]$_0$/[CuBr/PS8-dMbpy]$_0$/[soluble catalyst]$_0$ = 300:1:1:0.01; $[MMA]_0$ = 4.69 mol/L; soluble catalysts from stock solution in acetone; MMA/(toluene + anisole)/acetone = 1/1/0.07 v/v; temperature = 90 °C.

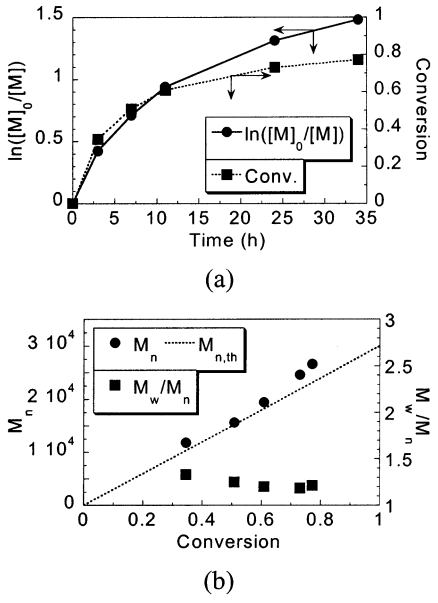

Figure 5. Kinetic plots (a) and evolution of M_n and M_w/M_n vs conversion (b) for the polymerization of MMA using the hybrid catalyst system composed of CuBr/PS8-dMbpy immobilized catalyst and Me_6TREN (without premetalation with $CuBr_2$). Polymerization conditions: $[MMA]_0$/[2-bromopropionitrile]$_0$/[CuBr/PS8-dMbpy]$_0$/$[Me_6TREN]_0$ = 300:1:1:0.01; $[MMA]_0$ = 4.69 mol/L; MMA/(toluene + anisole) = 1/1 v/v; temperature = 90 °C.

value is $\sim 10^7$ times higher than that with 2,2′-bipyridyne ($K_c \sim 10^{7.81}$).[48] Therefore, addition of only the Me_6-TREN ligand should provide for spontaneous abstraction of $CuBr_2$ from the immobilized catalyst to form in-situ the soluble $CuBr_2$/Me_6TREN deactivator. This would be an adventitious process improvement because liquid Me_6TREN is easy to handle and no precomplex formation step is necessary. Polymerization of MMA conducted with a hybrid catalyst formed with sole addition of Me_6TREN reached 80% in 24 h (Figure 5a) with a narrow molecular weight distribution ($M_w/M_n \sim$ 1.2, Figure 5b), a linear increase of molecular weight, and a good agreement between experimental/theoretical molecular weights (Figure 5b), confirming good control over the polymerization.

Hybrid Catalyst Systems with Different Sizes of Catalyst Support. Catalysts immobilized on different sizes of support bead were tested for preparation of the hybrid catalyst system. Poly(styrene-*co*-divinylbenzene) beads (PS beads) with an average diameter of 8 μm (5% divinylbenzene) and 50 μm (1% divinylbenzene) were compared using 1 mol % $CuBr_2$/Me_6TREN as a soluble catalyst component. No significant differences were found in molecular weight and molecular weight distribution. Both catalyst systems produced polymers with narrow molecular weight distributions ($M_w/M_n \sim 1.3$) and essentially the same molecular weight in good agreement with the theoretical values. The carrier with smaller particle size seems to offer some advantage in a batch agitated system, affording slightly faster polymerization rates without sacrificing control over the polymerization. However, this is offset because the smaller the particle, the more difficult it is to separate the catalyst from the polymerization medium through filtration or sedimentation.

Hybrid Catalyst Systems with Different Tethered Ligands Forming the Immobilized Catalyst. Immobilized catalysts were prepared with different tethered ligands, dMbpy and *N*,*N*-bis(2-pyridylmethyl)-2-hydroxyethylamine (bpa), using the 50 μm PS bead as support. The catalysts were tested for MMA polymerization with 1 mol % $CuBr_2$/Me_6TREN as the soluble catalyst component, and the results are shown in Figure 6. A faster polymerization was observed with bpa than with dMbpy as the attached ligand. The molecular weight distributions of the polymers formed with each catalyst system were almost identical, although the polymers from CuBr/PS50-bpa exhibited higher molecular weights than theoretical values especially at higher conversion, indicating loss of control over the polymerization.

The equilibrium constant (K) for the halogen exchange reaction with *N*,*N*-bis(2-pyridylmethyl)-2-hydroxyethylamine (bpa) was estimated using their chemical analogues (eq 3, BPOA = *N*,*N*-bis(2-pyridylmethyl)octylamine). Cyclic voltametry at 25 °C in acetonitrile afforded $K = K_{Me6TREN}/K_{BPOA} = 10^{4.4}$, which is slightly lower than that with 2,2′-bipyridine, $K = K_{Me6TREN}/K_{bpy} = 10^{5.6}$.[46] This suggests that $CuBr_2$/Me_6TREN is less efficiently regenerated, resulting in loss of control over the polymerization and a higher molecular weight.

$$CuBr_2/BPOA + CuBr/Me_6TREN \underset{K_{Me6TREN}}{\overset{K_{BPOA}}{\rightleftharpoons}} CuBr/BPOA + CuBr_2/Me_6TREN \quad (3)$$

Silica Supported CuBr/Diamine as an Immobilized Catalyst. Shen et al. used a CuBr/hexamethyltriethylenetetramine (HMTETA) adsorbed on silica as an immobilized ATRP catalyst.[34] When used for the

Table 4. Methyl Methacrylate, Methyl Acrylate, and Styrene Polymerization with CuBr/sil-dia, (CuBr/$CuBr_2$)/XVS43578, and Their Corresponding Hybrid Catalysts with $CuBr_2$/Me_6TREN[a]

expt no.	monomer	immobilized catalyst	hybrid ratio[b] (mol %)	polym time (h)	conv[c] (%)	M_n ($\times 10^3$)	M_n(th) ($\times 10^3$)	M_w/M_n
11	MMA	CuBr/sil-dia	0	9	41.6	25.5	12.5	1.96
12	MA	CuBr/sil-dia	0	20	32.1	14.7	8.3	2.00
13	sty	CuBr/sil-dia	0	20	56.1	64.7	17.5	2.21
14	MMA	CuBr/sil-dia	1	9	93.4	37.0	28.1	1.29
15	MMA	(CuBr/$CuBr_2$)/XVS43578	0	16	86.1	40.4	25.9	3.23
16	MMA	(CuBr/$CuBr_2$)/XVS43578	3	18	88.8	39.8	26.6	1.49

[a] Polymerization conditions: initiator = 2-bromopropionitrile except for expt no. 13; for expt no. 11, $[MMA]_0/[I]_0/[CuBr/sil\text{-}dia]_0 = 300:1:1$, $[MMA]_0 = 4.69$ mol/L, MMA/toluene = 1/1 v/v, temperature = 90 °C; for expt no. 12, $[MA]_0/[I]_0/[CuBr/sil\text{-}dia]_0 = 300:1:1$, $[MA]_0 = 5.56$ mol/L, MA/(toluene + anisole) = 1/1 v/v, temperature = 70 °C; for expt no. 13, initiator = 1-bromoethylbenzene, $[styrene]_0/[I]_0/[CuBr/sil\text{-}dia]_0 = 300:1:1$, $[styrene]_0 = 4.36$ mol/L, sty/(chlorobenzene + anisole) = 1/1 v/v, temperature = 110 °C; for expt no. 14, $[MMA]_0/[I]_0/[CuBr/sil\text{-}dia]_0/[CuBr_2/Me_6TREN]_0 = 300:1:1:0.01$, $CuBr_2/Me_6$TREN from stock solution in acetone, $[MMA]_0 = 4.67$ mol/L, MMA/toluene/acetone = 1/0.90/0.10 v/v/v, temperature = 90 °C; for expt no. 15, $[MMA]_0/[I]_0/[(CuBr/CuBr_2)/XVS43578]_0 = 300:1:1$, $[MMA]_0 = 4.69$ mol/L, MMA/toluene = 1/1 v/v, temperature = 90 °C; for expt no. 16, $[MMA]_0/[I]_0/[(CuBr/CuBr_2)/XVS43578]_0/[CuBr_2/Me_6TREN]_0 = 300:1:1:0.03$, $CuBr_2/Me_6$TREN from stock solution inacetone, $[MMA]_0 = 4.68$ mol/L, MMA/toluene/acetone = 1/0.68/0.32 v/v/v, temperature = 90 °C. [b] $[CuBr_2/Me_6TREN]_0/[CuBr/bpy$ immobilized on PS bead$]_0$ (mol %). [c] Conversion determined by GC.

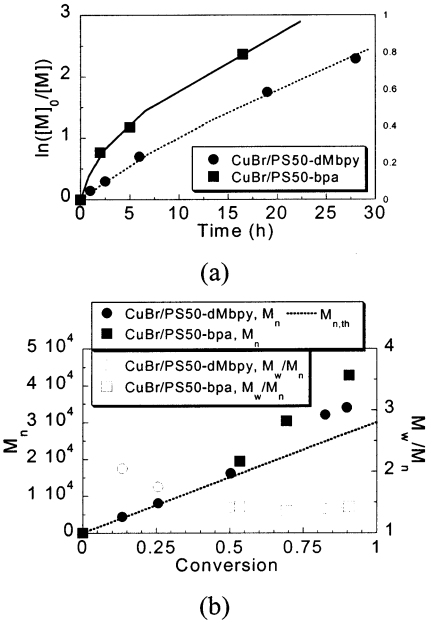

Figure 6. Kinetic plots (a) and the evolution of M_n and M_w/M_n vs conversion (b) for the polymerization of MMA using the hybrid catalyst system composed of $CuBr_2$/Me_6TREN as a soluble catalyst constituent and the immobilized catalysts with different ligands: CuBr/PS50-dMbpy (● or ○); CuBr/PS50-bpa (■ or □). Polymerization conditions: $[MMA]_0/[2\text{-bromopropionitrile}]_0/[\text{immobilized catalyst}]_0/[CuBr_2/Me_6TREN]_0 = 300:1:1:0.01$; $[MMA]_0 = 4.69$ mol/L; $CuBr_2/Me_6$TREN from stock solution in acetone; MMA/(toluene + anisole)/acetone = 1/1/0.14 v/v/v; temperature = 90 °C.

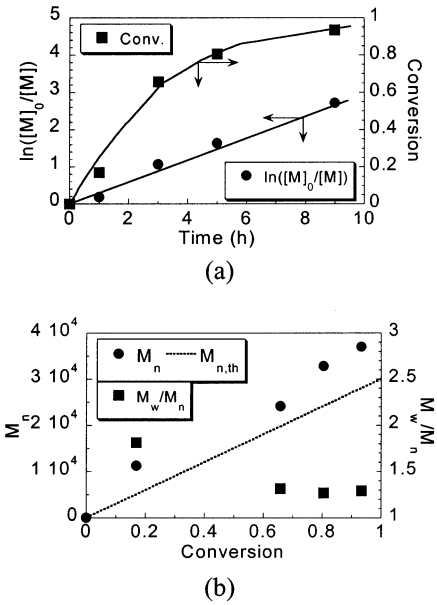

Figure 7. Kinetic plots (a) and the evolution of M_n and M_w/M_n vs conversion (b) for the polymerization of MMA (experiment 14 in Table 4) with the (CuBr/sil-dia)/($CuBr_2$/Me_6TREN) hybrid catalyst system. Polymerization conditions: $[MMA]_0/[2\text{-bromopropionitrile}]_0/[CuBr/sil\text{-}dia]_0/[CuBr_2/Me_6TREN]_0 = 300:1:1:0.01$; $[MMA]_0 = 4.69$ mol/L; $CuBr_2/Me_6$TREN from stock solution in acetone; MMA/toluene/acetone = 1/0.90/0.10 v/v/v; temperature = 90 °C.

polymerization of 33% MMA in solution, the polymerization followed first-order kinetics with low polydispersity of the polymer, although the molecular weights were different from the theoretical values. However, the use of purely physically adsorbed catalyst on silica may result in catalyst-leaching during the polymerization, which would significantly increase the amount of residual Cu in polymer. We evaluated an aliphatic diamine complexed with CuBr covalently attached to silica (CuBr/sil-dia, CuBr/*N*,*N*,*N*′-trimethyl-*N*′-[3-(trimethoxysilylporpoxycarbonyl)ethyl]ethylenediamine**)** for ATRP of MMA, MA, and styrene. Experiments 11−13 in Table 4 show that the polymerization resulted in low conversion and a large difference between experimental/theoretical molecular weights, along with a broad molecular weight distribution ($M_w/M_n \sim 2.0$), indicating that the level of control over the polymerizations using this tethered ligand CuBr/sil-dia catalyst was poor. However, the addition of 1 mol % of a soluble catalyst ($CuBr_2$/Me_6TREN) significantly improved the level of the control over MMA polymerization (experiment 14 in Table 4, Figure 7). Polymer with a narrow molecular weight distribution ($M_w/M_n \sim 1.3$) and good agreement between experimental/theoretical molecular weights was formed (Figure 7b). Linear semilogarithmic kinetic behavior (Figure 7a) with high conversion (~93.4% in 9 h) was obtained. This was faster than polymerization with the (CuBr/PS8-dMbpy)/($CuBr_2$/Me_6TREN) hybrid catalyst system.

Use of DOWEX Anion-Exchange Resin as Support for an Immobilized Catalyst. Macrorecticular PS beads functionalized with *N*,*N*-bis(2-pyridylmethyl)-ethylamine (XVS43578) in the form of sulfate salts are commercially available from DOW (DOWEX anion-exchange resin). Neutralization of this resin with 1 M NaOH followed by washing and complexation with $CuBr/CuBr_2$ (8/2 mol/mol) afforded an immobilized

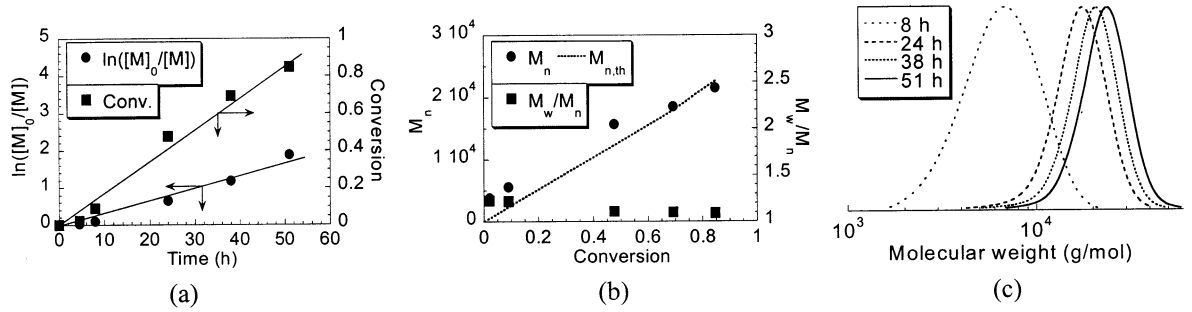

Figure 8. Kinetic plots (a), the evolution of M_n and M_w/M_n vs conversion (b), and GPC traces (c) for the polymerization of MA (experiment 8 in Table 2) using the (CuBr/PS8-dMbpy)/($CuBr_2$/Me_6TREN) hybrid catalyst system. Polymerization conditions: $[MA]_0/[2\text{-bromopropionitrile}]_0/[CuBr/PS8\text{-}dMbpy]_0/[CuBr_2/Me_6TREN]_0$ = 300:1:1:0.01; $CuBr_2/Me_6$TREN from stock solution in acetone; $[MA]_0$ = 5.55 mol/L; MA/toluene/acetone = 1/0.87/0.13 v/v/v; temperature = 70 °C.

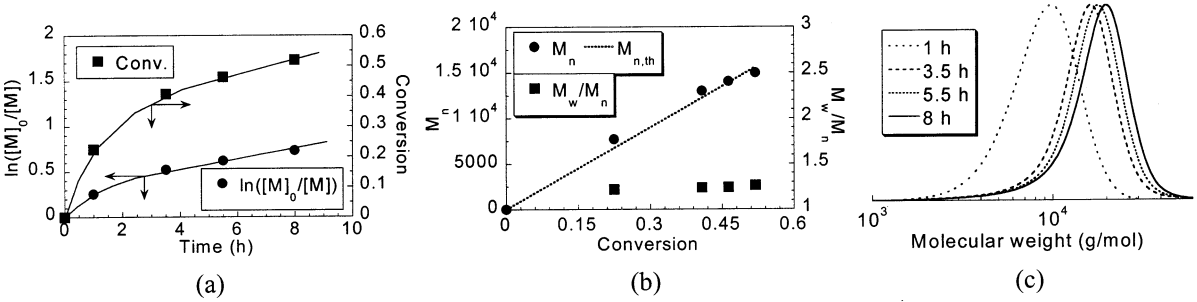

Figure 9. Kinetic plots (a), the evolution of M_n and M_w/M_n vs conversion (b), and GPC traces (c) for the polymerization of styrene (experiment 10 in Table 2) using the (CuBr/PS8-dMbpy)/($CuBr_2$/Me_6TREN) hybrid catalyst system. Polymerization conditions: $[styrene]_0/[1\text{-bromoethylbenzene}]_0/[CuBr/PS8\text{-}dMbpy]_0/[CuBr_2/Me_6TREN]_0$ = 300:1:1:0.01; $CuBr_2/Me_6$TREN from stock solution in acetone; $[styrene]_0$ = 4.36 mol/L; styrene/chlorobenzene/acetone = 1/0.75/0.12 v/v/v; temperature = 110 °C.

ATRP catalyst. The catalysts were tested for MMA polymerization, and the results are summarized in Table 4. High conversion (~86.1%) was obtained at 16 h, but the polymerization was not controlled, judging from the high polydispersity (M_w/M_n = 3.23) and large difference between theoretical and experimental molecular weights. However, the addition of $CuBr_2/Me_6$TREN (3 mol % versus immobilized catalyst) provided polymers with a relatively narrower molecular weight distribution (M_w/M_n = 1.49, experiment 16 in Table 4), indicating better control over the polymerization of MMA. A linear increase of molecular weight was observed for all conversions, although differences between theoretical and experimental molecular weights were noted. The semilogarithmic kinetic plot exhibited a linear increase of conversion with time, resulting in 88.8% conversion after 18 h (experiment 16 in Table 4). Presumably, the combination of bpa ligand on the immobilized catalysts and larger particle size limited the efficiency of the immobilized catalyst.

These results demonstrated the versatility of the hybrid catalyst concept. Regardless of the physicochemical properties of the carrier and ligand, significant improvements over control over the polymerization were seen after the addition of $CuBr_2/Me_6$TREN in part per million levels. The successful use of commercially available resin, DOWEX XVS43578, as support for the catalyst is expected to afford an expedient way for the successful scaling-up of supported catalyst ATRP.

Polymerization of Methyl Acrylate and Styrene with the (CuBr/PS8-dMbpy)/($CuBr_2$/Me_6TREN) Hybrid Catalyst. Methyl acrylate (MA) polymerization was conducted with the hybrid catalyst system containing 1 mol % $CuBr_2/Me_6$TREN versus CuBr/PS8-dMbpy. The results are shown in experiment 8 in Table 2 and Figure 8. A well-controlled polymerization was observed up to high conversion (~85%), and the semilogarithmic kinetic plot (Figure 8a) displayed a linear increase of conversion with time. The experimental and theoretical molecular weights were essentially identical for all conversions (experiment 8 in Table 2 and Figure 8b). The GPC traces shown in Figure 8c demonstrated symmetrical molecular weight distributions with clear shifts to the high molecular weight region with conversion.

Although k_p for acrylates (e.g. 27 700 L mol^{-1} s^{-1} in bulk at 70 °C)[49−51] is much higher than that for MMA (1050 L mol^{-1} s^{-1} in bulk at 70 °C),[50,52] and this usually leads to higher polydispersities for polyacrylates than for polymethacrylates (eq 4[8]), a narrower molecular weight distribution ($M_w/M_n \sim 1.09$, experiment 8, Table 2) was observed for MA (Figure 10b) with the hybrid catalyst system. This result can be attributed to the high k_d of $CuBr_2/Me_6$TREN for the acrylate radical and to the relatively constant deactivator concentration in this hybrid catalyst system.

$$M_w/M_n = 1 + ([\text{initiator}]_0 k_p/k_d[\text{deactivator}])(2/p - 1) \quad (4)$$

Good control over the polymerization of styrene was also observed with 1 mol % $CuBr_2/Me_6$TREN versus CuBr/PS8-dMbpy (Figure 9, experiment 10 in Table 2). The kinetic plot exhibited a first-order kinetics with a slightly faster initial rate (Figure 11a). The theoretical and experimental molecular weights showed very good agreements with a narrow molecular weight distribution ($M_w/M_n \sim 1.2$, Figure 9b). The GPC traces exhibited clear shifts to the high molecular weight region with conversion. No specific broadening over the traces was observed, although some tailing in the low molecular weight region existed. However, conversions higher than

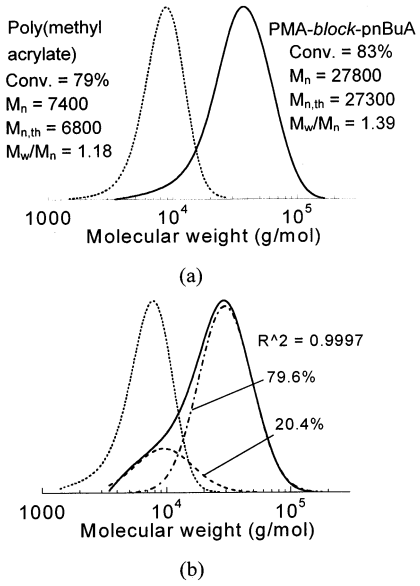

Figure 10. GPC traces for the preparation of poly(methyl acrylate)-*block*-poly(*n*-butyl acrylate) through the chain extension polymerization (a) and their number distribution curves (b). The number distribution GPC curve of poly(methyl acrylate)-*block*-poly(*n*-butyl acrylate) is deconvolved into two Gaussian distribution curves using Origin 6.1 software.

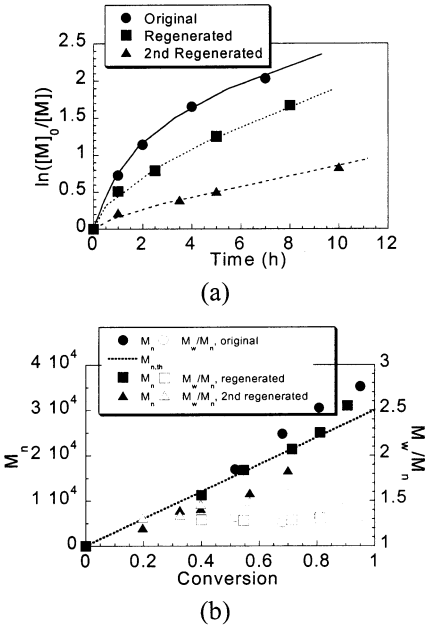

Figure 11. Kinetic plots (a) and the evolution of M_n and M_w/M_n vs conversion (b) for the polymerization of MMA using the (CuBr/PS8-dMbpy)/($CuBr_2$/Me_6TREN) hybrid catalyst system with original, regenerated, and second regenerated immobilized catalyst. Polymerization conditions: $[MMA]_0/[2\text{-bromopropionitrile}]_0/[CuBr/PS8\text{-}dMbpy]_0/[CuBr_2/Me_6TREN]_0 = 300:1:1:0.01$; $[MMA]_0 = 4.69$ mol/L; $CuBr_2/Me_6$TREN from stock solution in acetone; MMA/(toluene + anisole)/acetone = 1/1/0.14 v/v/v; temperature = 90 °C.

60% were difficult to attain, and the reason is presently not clear. At higher polymerization temperature (120 °C), higher conversion (~80%) was seen after 48 h, although a high molecular weight side peak (~1×10^5 g/mol) appeared after 20 h of polymerization.

Polymerization of MMA and MA to Lower Degrees of Polymerization. PMMA and PMA with lower degrees of polymerization ($DP_n = 100$) were targeted and prepared with the hybrid catalyst system (1 mol % $CuBr_2$/Me_6TREN versus CuBr/PS8-dMbpy). The results are summarized in experiments 6 and 9 in Table 2. Conversions higher than 96% were obtained in 6 h. The polymerizations were 5−10 times faster (compared at 50% conversion) than those when the targeted degree of polymerization was 300 (experiments 4 and 8). This is in agreement with the higher initiator and catalyst concentrations. Good agreements between theoretical and experimental molecular weights were observed (Table 2, experiments 6 and 9), but the molecular weight distributions were slightly broader than those for the polymers in experiments 4 and 8, probably because of the lower number of exchange reactions between dormant and active species.

Preparation of Block Copolymers through Chain Extension. Preparation of a pMA-*block*-pnBuA copolymer was conducted (Figure 10) to evaluate the "living" character of the polymerization system. The pMA segment was prepared by the (CuBr/PS8-dMbpy)/($CuBr_2$/Me_6TREN) hybrid catalyst system with a targeted degree of polymerization of 100. After a level of conversion of 79% was reached, ^{n}BuA was added to prepare an A−B tapered block copolymer. As shown in Figure 10a, the GPC traces exhibited a clear shift to higher molecular weight as the polymer chain extended from pMA to pnBuA. The narrow molecular weight distribution of the block copolymer ($M_w/M_n \sim 1.39$) and a good agreement between experimental and theoretical molecular weight demonstrate a clean chain extension reaction and the living character of the polymerization system. The corresponding number average distribution curve against molecular weight (Figure 10b), obtained by dividing signal intensities from the refractometer by molecular weight, demonstrated that >80% of the pMA chains retained the active chain end functionality, allowing for chain extension to form the block copolymerization. This value could be even higher, since the refractive index difference between pMA and THF is larger than that between p^{n}BuA and THF.[53]

Residual Cu in the Polymer. After sedimentation, or simple filtration of the polymerization mixture through a Gelman Acrodisc 0.2 μm PTFE filter, the immobilized catalyst was efficiently removed, affording a clear, colorless polymer solution. Solvent casting of the polymer solution afforded a clear, transparent polymer film. The residual concentration of Cu in the polymer films was measured by inductively coupled plasma (ICP) analysis. The results are summarized in Table 2.

Residual Cu was not detected by ICP in the polymer prepared using the CuBr/PS8-dMbpy immobilized catalyst (<1 ppm, experiment 1 in Table 2), indicating that leaching of the catalyst from the immobilized catalyst during the polymerization was negligible. To confirm this result, an extraction experiment was performed for the CuBr/PS8-dMbpy catalyst complex using degassed MMA/toluene (1/1 v/v) as a solvent. This resulted in no detectable Cu signals by UV−visible spectrometer, even when bis(cyclohexanone)oxalydihydrazone, which forms a strong blue complex with Cu^{II}, was added as a colorant.

The levels of residual Cu in the polymer obtained from polymerizations conducted with nonsupported (CuBr/$CuBr_2$)/Me_6TREN catalyst were very high (1730 ppm, experiment 2 in Table 2), because essentially the entire Cu complex should remain in the polymer (theoretical value, 3026 ppm, experiment 2 in Table 2). Experimentally, the residual amount of copper in the polymer was

Table 5. Measured Copper and Ligand Levels in the Original (CuBr/PS8-dMbpy) Catalyst and the First and Second Regenerated Catalysts and Their MMA Polymerization Behavior[a]

expt no.	immobilized catalyst	Cu content[b] (mol-Cu/g-cat)	ligand content[c] (mol-ligand/g-cat)	Cu content decrease[d] (%)	ligand content decrease[d] (%)	polym time (h)	conv[e] (%)	M_n ($\times 10^3$)	M_n(th) ($\times 10^3$)	M_w/M_n
17	CuBr/PS8-dMbpy	7.427×10^{-4}	1.310×10^{-3}	0	0	24	95.1	38.1	28.5	1.34
18	1st regenerated	6.609×10^{-4}	7.990×10^{-4}	11.0	39.0	20	90.6	31.0	27.2	1.41
19	2nd regenerated	4.752×10^{-4}	5.460×10^{-4}	36.0	58.3	29	70.0	16.7	21.0	1.58

[a] Polymerization conditions: catalyst = (CuBr/PS8-dMbpy)/($CuBr_2$/Me_6TREN) hybrid catalyst system; $[MMA]_0/[2\text{-bromopropionitrile}]_0/[CuBr/PS8\text{-}dMbpy]_0/[CuBr_2/Me_6TREN]_0 = 300:1:1:0.01$; $[MMA]_0 = 4.69$ mol/L; $CuBr_2/Me_6$TREN from stock solution in acetone; MMA/(toluene + anisole)/acetone = 1/1/0.14 v/v/v; temperature = 90 °C. [b] Copper (Cu) content in the immobilized catalyst determined by inductively coupled plasma (ICP) analysis. [c] Ligand content in the immobilized catalyst determined by C, H, N analysis. [d] The percentage of the reduction of the Cu and ligand content in the immobilized catalyst compared to that in the original catalyst. [e] Conversion determined by GC.

less than the theoretical value because of the incomplete dissolution of CuBr/Me_6TREN and $CuBr_2/Me_6$TREN in the reaction medium.

The residual amounts of Cu in the polymer prepared with hybrid catalysts with varying levels of soluble components were significantly lower with the catalysts comprising ratios of 3, 1, and 0.3% Me_6TREN, giving values of 107, 27, and 15 ppm, respectively. These values are slightly higher than, but relatively close to, the theoretical values (76, 24, and 6 ppm, respectively). For the polymers from experiments 6, 8, 9, and 10, the concentrations of residual Cu were also close to the theoretical value regardless of the type of the monomer. The residual concentration of Cu in polymer prepared from the hybrid catalyst with 1 mol % $CuBr_2/Me_6$TREN using the larger PS bead support and silica afforded 33 and 32 ppm, which are also very close to the theoretical values (24 and 22 ppm).

The residual amount of Cu in the polymer could be further reduced through the introduction of water during the polymerization. Polymerization of MMA in the presence of toluene/water (84/16 v/v) solvent reduced the residual amount of Cu in the polymer to 3 ppm (theoretical value, 29 ppm), although this was accomplished with some loss of the level of the control over the polymerization because of the high partitioning coefficient of Cu^{II} species preferentially to the water phase ($M_n = 43\,000$, $M_{n,th} = 21\,000$, $M_w/M_n = 1.79$).

Regeneration of the Immobilized Catalyst. The color of the CuBr/PS8-dMbpy immobilized catalyst turned from dark brown to light brown during the polymerization, indicating accumulation of Cu^{II} during the polymerization, probably as a result of termination reactions. Regeneration of the catalyst is therefore necessary prior to catalyst reuse. The addition of the Cu^0 (copper powder or wire) has been shown to slowly reduce the concentration of Cu^{II} by an electron-transfer process, generating two Cu^I species.[54] Catalyst regeneration was attempted by exposing the used catalyst to zerovalent metal (Cu^0) in the presence of a soluble ligand to act as a shuttle between the two solid species.

After a polymerization reaction, the CuBr/PS8-dMbpy immobilized catalyst was collected and washed thoroughly with degassed THF and regeneration was attempted in the presence of THF at 60 °C. Initially, Cu^0 wire alone was employed as the reducing agent. The color of the PS8-dMbpy turned from light brown to dark brown in 24 h. However, when the regenerated immobilized catalyst was used in a hybrid catalyst system containing 1 mol % $CuBr_2/Me_6$TREN, the catalyst afforded low conversion (36.3% in 19 h) in MMA polymerization. A more effective regeneration reaction was accomplished by addition of 10 mol % $CuBr_2/Me_6$TREN versus immobilized catalyst to act as a halogen-delivery messenger between Cu^0 and $CuBr_2$/PS8-dMbpy in the regeneration step. The color of the immobilized catalyst turned to dark brown in 6 h. The $CuBr_2/Me_6$TREN was adopted as a halogen-delivery messenger, since the electron-transfer reaction between two solid components would be expected to be very slow. Cu^0 reacts with $CuBr_2/Me_6$TREN and is converted to Cu^IBr while the $CuBr_2/Me_6$TREN is reduced to CuBr/Me_6TREN. The CuBr/Me_6TREN then reduces $CuBr_2$/PS8-dMbpy to CuBr/PS8-dMbpy and is reconverted to $CuBr_2/Me_6$TREN, thereby completing the regeneration halogen transfer cycle.

However, the activity of regenerated immobilized catalyst for polymerization of MMA in a hybrid catalyst system decreased with every regeneration step (Table 5 and Figure 11). The polymer prepared from each successive regenerated immobilized catalyst exhibits slightly lower molecular weight and broader molecular weight distribution (Table 5 and Figure 11). This behavior can be attributed to an incomplete regeneration reaction, which would lead to accumulation of Cu^{II} in the immobilized catalyst,[36] resulting in lower activity. However, another explanation is that "attached" polymer may reduce the access of monomers to the catalyst. Polymer could remain on the immobilized catalyst through pure physical adsorption of polymers or as a result of a *grafting-from* polymerization from a residual benzyl chloride initiating site on the PS8-dMbpy catalyst. Both phenomena may result in formation of a polymer coating around the catalyst particle, hindering the approach of the reagents to the tethered catalyst, reducing the activity, and leading to an uncontrolled polymerization. The physical entrapment of the polymer may result from chain entanglement or slow diffusion of polymer from inside the pores during the washing steps. To check whether this was occurring, the immobilized catalyst was weighed before and after polymerization. The used catalyst was washed eight times with THF, and the weight of the immobilized catalyst was found to have increased by 27.8% (0.113 g before polymerization, 0.144 g after polymerization). The concentration of Cu and ligand in the catalyst measured by ICP after the polymerization and washing steps decreased by 13.7% and 27.0%, respectively. These values were relatively close to an 11.0% and 39.0% reduction of Cu and ligand content after the regeneration step (Table 5), suggesting that the reductions of the measured Cu and ligand levels in the regenerated immobilized catalysts are probably due to polymer accumulation. The weight of CuBr/sil-dia catalyst, which lacks any initiating sites, also increased after polymerization, by 10.8%. This value is lower than that seen for the CuBr/PS8-dMbpy catalyst. These observations suggest that the decrease in concentration of the ligand

and Cu content in the regenerated immobilized catalyst may originate from both a *grafting-from* polymerization and chain entrapment inside pores present in the support.

In-situ regeneration was attempted by conducting the polymerization in the presence of Cu^0, that should slowly convert Cu^{II} to Cu^I. When a MMA polymerization was carried out in the presence of Cu^0 powder, it resulted in a much slower rate of polymerization (15% conversion in 45 h) and produced polymers possessing broader molecular weight distributions ($M_w/M_n = 1.4$). A better result was achieved using Cu^0 wire (experiment 7 in Table 2). The polymerization was faster, leading to 92.5% conversion in 5.5 h. However, the experimental molecular weight was higher than the theoretical value with the high polydispersity ($M_w/M_n = 1.58$). This observation can be attributed to a reduction in the concentration of $CuBr_2$/Me_6TREN to CuBr/Me_6TREN by the Cu^0 wires, while Cu^0 wire is converted to a soluble Cu^IBr species. Removal of Cu^{II} and generation of Cu^I enhanced the polymerization rate (eq 5) and increased the polydispersity (eq 4) because of a reduction of the concentration of the deactivator in solution. Because the Cu^0 wire is gradually converted to Cu^IBr species that become soluble in the polymerization medium, the residual amount of Cu in the polymer was found to be much higher than expected (63 ppm, experiment 7 in Table 2).

Conclusion

A hybrid catalyst system for ATRP, composed of an immobilized catalyst and a small amount of soluble catalyst, was investigated for ATRP. The level of control over the polymerization of vinyl monomers was significantly improved by the addition of part per million quantities of a secondary soluble catalyst to a solid supported immobilized catalyst. The role of the soluble catalyst component is to facilitate an effective deactivation process by delivering the halogen from the solid immobilized catalyst to growing polymeric radicals, thus overcoming diffusion barriers. The use of a hybrid catalyst system afforded a high conversion of monomers to polymers displaying a predetermined molecular weight and narrow molecular weight distribution. We have shown that $CuBr_2$/Me_6TREN, which is a more reducing soluble catalyst, was advantageous as the soluble catalyst component, since this characteristic accelerated the halogen exchange reaction. A range of suitable immobilized catalysts can be constructed from different supports, different attached ligands, and encompassing particles of different sizes and pore structures. The successful controlled polymerization of vinyl monomers such as MMA, MA, and styrene, providing polymers with various degrees of polymerization and different architectures (such as block copolymers), proves the versatility and living character of the system. In the batch polymerization system examined, the immobilized catalyst was removed from the polymerization media by simple filtration or sedimentation, affording a colorless transparent polymer solution with a salient reduction of the residual transition metal in the final polymer products. Although improvements on the regeneration process are still required, we have shown that a hybrid catalyst system provides a simple, versatile, and efficient ATRP process, which may open a new route for the commercialization of ATRP.

Acknowledgment. We greatly appreciate the financial support from the U.S. Environmental Protection Agency, the National Science Foundation (DMR-0090409), and the ATRP/CRP Consortia. Dr. S. Gaynor is acknowledged for the donation of DOWEX resin. Dr. James Spanswick is acknowledged for many valuable comments and other contributions to this project.

References and Notes

(1) Matyjaszewski, K., Ed. *Controlled Radical Polymerization*; American Chemical Society: Washington, DC, 1998; Vol. 685.
(2) Matyjaszewski, K., Ed. *Controlled/Living Radical Polymerization: progress in ATRP, NMP, and RAFT*; The American Chemical Society: Washington, DC, 2000; Vol. 768.
(3) Wang, J.-S.; Matyjaszewski, K. *J. Am. Chem. Soc.* **1995**, *117*, 5614.
(4) Sawamoto, M.; Kamigaito, M. *Chemtech* **1999**, *29*, 30−38.
(5) Matyjaszewski, K. *Chem. Eur. J.* **1999**, *5*, 3095−3102.
(6) Patten, T. E.; Matyjaszewski, K. *Acc. Chem. Res.* **1999**, *32*, 895−903.
(7) Patten, T. E.; Matyjaszewski, K. *Adv. Mater.* **1998**, *10*, 901.
(8) Matyjaszewski, K.; Xia, J. *Chem. Rev.* **2001**, *101*, 2921.
(9) Coessens, V.; Pintauer, T.; Matyjaszewski, K. *Prog. Polym. Sci.* **2001**, *26*, 337−377.
(10) Patten, T. E.; Xia, J.; Abernathy, T.; Matyjaszewski, K. *Science* **1996**, *272*, 866−868.
(11) Xia, J.; Matyjaszewski, K. *Macromolecules* **1997**, *30*, 7697.
(12) Xia, J.; Gaynor, S. G.; Matyjaszewski, K. *Macromolecules* **1998**, *31*, 5958.
(13) Xia, J.; Zhang, X.; Matyjaszewski, K. *ACS Symp. Ser.* **2000**, *760*, 207−223.
(14) Kickelbick, G.; Matyjaszewski, K. *Macromol. Rapid Commun.* **1999**, *20*, 341−346.
(15) Matyjaszewski, K.; Gobelt, B.; Paik, H.-j.; Horwitz, C. P. *Macromolecules* **2001**, *34*, 430.
(16) Gromada, J.; Matyjaszewski, K. *Macromolecules* **2001**, *34*, 7664−7671.
(17) Matyjaszewski, K.; Pintauer, T.; Gaynor, S. *Macromolecules* **2000**, *33*, 1476−1478.
(18) Xia, J.; Johnson, T.; Gaynor, S.; Matyjaszewski, K.; DeSimone, J. *Macromolecules* **1999**, *32*, 4802.
(19) Carmichael, A. J.; Haddleton, D. M.; Bon, S. A. F.; Seddon, K. R. *Chem. Commun.* **2000**, 1237.
(20) Sarbu, T.; Matyjaszewski, K. *Macromol. Chem. Phys.* **2001**, *202*, 3371.
(21) Biedron, T.; Kubisa, P. *Macromol. Rapid Commun.* **2001**, *22*, 1237−1242.
(22) Gaynor, S.; Qiu, J.; Matyjaszewski, K. *Macromolecules* **1998**, *31*, 5951.
(23) Qiu, J.; Pintauer, T.; Gaynor, S. G.; Matyjaszewski, K.; Charleux, B.; Vairon, J.-P. *Macromolecules* **2000**, *33*, 7310−7320.
(24) Qiu, J.; Gaynor, S.; Matyjaszewski, K. *Macromolecules* **1999**, *32*, 2872.
(25) Qiu, J.; Charleux, B.; Matyjaszewski, K. *Prog. Polym. Sci.* **2001**, *26*, 2083-2134.
(26) Haddleton, D. M.; Jackson, S. G.; Bon, S. A. F. *J. Am. Chem. Soc.* **2000**, *122*, 1542.
(27) Angot, S.; Ayres, N.; Bon, S. A. F.; Haddleton, D. M. *Macromolecules* **2001**, *34*, 768.
(28) Von Werne, T.; Patten, T. E. *J. Am. Chem. Soc.* **1999**, *121*, 7409−7410.
(29) Pyun, J.; Matyjaszewski, K.; Kowalewski, T.; Savin, D.; Patterson, G.; Kickelbick, G.; Huesing, N. *J. Am. Chem. Soc.* **2001**, *123*, 9445−9446.
(30) Matyjaszewski, K.; Miller, P. J.; Shukla, N.; Immaraporn, B.; Gelman, A.; Luokala, B. B.; Siclovan, T. M.; Kickelbick, G.; Vallant, T.; Hoffmann, H.; Pakula, T. *Macromolecules* **1999**, *32*, 8716−8724.
(31) Haddleton, D. M.; Kukulj, D.; Radigue, A. P. *Chem. Commun.* **1999**, 99.
(32) Haddleton, D. M.; Duncalf, D. J.; Kukulj, D.; Radigue, A. P. *Macromolecules* **1999**, *32*, 4769.
(33) Kickelbick, G.; Paik, H.-j.; Matyjaszewski, K. *Macromolecules* **1999**, *32*, 2941−2947.
(34) Shen, Y.; Zhu, S.; Zeng, F.; Pelton, R. H. *Macromolecules* **2000**, *33*, 5427.
(35) Shen, Y.; Zhu, S.; Pelton, R. *Macromol. Rapid Commun.* **2000**, *21*, 956.
(36) Shen, Y.; Zhu, S.; Zeng, F.; Pelton, R. *Macromol. Chem. Phys.* **2000**, *201*, 1387.

(37) Matyjaszewski, K.; Paik, H.-j.; Zhou, P.; Diamanti, S. J. *Macromolecules* **2001**, *34*, 5125.
(38) Kroell, R.; Eschbaumer, C.; Schubert, U. S.; Buchmeiser, M. R.; Wurst, K. *Macromol. Chem. Phys.* **2001**, *202*, 645.
(39) Shen, Y.; Zhu, S.; Pelton, R. *Macromolecules* **2001**, *34*, 5812.
(40) Liou, S.; Rademacher, J. T.; Malaba, D.; Pallack, M. E.; Brittain, W. J. *Macromolecules* **2000**, *33*, 4295.
(41) Shen, Y.; Zhu, S.; Pelton, R. *Macromolecules* **2001**, *34*, 3182.
(42) Hong, S. C.; Paik, H.-j.; Matyjaszewski, K. *Macromolecules* **2001**, *34*, 5099.
(43) Matyjaszewski, K.; Patten, T. E.; Xia, J. *J. Am. Chem. Soc.* **1997**, *119*, 674.
(44) Queffelec, J.; Gaynor, S. G.; Matyjaszewski, K. *Macromolecules* **2000**, *33*, 8629.
(45) Pintauer, T.; Matyjaszewski, K. Unpublished results. *K* was estimated for soluble/soluble catalyst pairs using UV−vis spectrometry through multiwavelength analysis by resolving the spectra into individual spectral components to obtain the concentration of each species. A study to measure the *K* values for immobilized/soluble catalyst pairs is now under investigation.
(46) Qiu, J.; Matyjaszewski, K.; Thouin, L.; Amatore, C. *Macromol. Chem. Phys.* **2000**, *201*, 1625: $\ln K = nFE/RT$, $E = 0.06 \log K$ at room temperature, $\Delta E = E_{1/2}(Cu^{II}/bpy) - E_{1/2}(Cu^{II}/Me_6TREN) = 0.335$ V, where $E_{1/2}$ are redox potentials; from the above equation $K \sim 10^5$.
(47) Golub, G.; Lashaz, A.; Cohen, H.; Paoletti, P.; Bencini, A.; Valtancoli, B.; Meyerstein, D. *Inorg. Chim. Acta* **1997**, *255*, 111.
(48) Pintauer, T. Unpublished results. The complex formation equilibrium constant for the stepwise complex formation of 2,2′-bipyridyl (2.0×10^{-3} mol/L) with $Cu(CF_3SO_3)_2$ (1.0×10^{-3} mol/L) in aqueous solution was measured using UV−vis spectrometry through multiwavelength analysis by resolving the spectra into individual spectral components to obtain the concentration of each species.
(49) Buback, M.; Kurz, C. H.; Schmaltz, C. *Macromol. Chem. Phys.* **1998**, *199*, 1721.
(50) Herk, A. M. V. *Macromol. Theory Simul.* **2000**, *9*, 433.
(51) Beuermann, S.; Buback, M. *Prog. Polym. Sci.* **2002**, *27*, 191−254.
(52) Beuermann, S.; Buback, M.; Davis, T. P.; Gilbert, R. G.; Hutchinson, R. A.; Olaj, O. F.; Russell, G. T.; Schweer, J.; Herk, A. M. V. *Macromol. Chem. Phys.* **1997**, *198*, 1545.
(53) Brandrup, J., Immergut, E. H., Eds. *Polymer Handbook*, 3rd ed.; Wiley: New York, 1989.
(54) Matyjaszewski, K.; Coca, S.; Gaynor, S. G.; Wei, M.; Woodworth, B. E. *Macromolecules* **1997**, *30*, 7348.

MA020054O